Diffraction of Neutrons by Gas Molecules

A THESIS

Submitted in Partial Fulfilment of the
Requirements for the Degree of Doctor of Philosophy
in the Faculty of Graduate Studies and Research,
McGill University

by

Norman Z. Alcock

April, 1949

ACKNOWLEDGMENTS

The author would like to thank Dr. B. W. Sargent who suggested the problem and under whose direction the research was performed, and Dr. D. G. Hurst not only for making available the crystal spectrometer used in the experiment, but also for his many helpful discussions and suggestions. Acknowledgments are also due many individuals on the staff of the National Research Council Laboratories at Chalk River for their considerable expert assistance.

The author wishes to express to Dr. J. S. Foster and Dr. A. Norman Shaw of McGill University his appreciation of their liberality in allowing this work to be performed at Chalk River.

SUMMARY

A monokinetic beam of neutrons (0.07 e.v.) has been scattered by a gas, and the angular dependence of scattering measured over the range 0° to 90°. This is believed to be the first measurement of neutrons diffracted by gas molecules.

The experiments were performed with a modified neutron crystal spectrometer using a beam of neutrons from the Chalk River pile. The gases studied, CO_2 and O_2, were at room temperature and approximately 60 atmospheres pressure.

Observed intensity distributions are compared with calculated patterns. The latter are based on classical interference theory, so take no account of inelastic scattering.

Good angular agreement of interference peaks is found for both gases. Good relative intensity agreement is found for O_2, but the measured intensity for CO_2 falls below the calculated curve at small angles. A possible reason for this is given.

TABLE OF CONTENTS

1. GENERAL INTRODUCTION

X-ray diffraction by the free molecules of a gas was predicted in 1915, and measured in 1929. Two years later, interference patterns from a gas were also observed for electrons. The experiments described in this thesis are believed to be the first measurements of neutrons diffracted by a gas.

The Chalk River pile and a neutron crystal spectrometer provided the required monokinetic beam of slow neutrons. This beam was scattered by the gas, and its resultant angular distribution measured with a BF_3 neutron counter, revolving about the gas sample. Cadmium irises prevented the counter from "seeing" the sections of high pressure gas chamber struck by the incident beam, but despite this precaution, background and true counts were approximately equal.

By this method the angular distributions of scattered neutrons from carbon dioxide and oxygen have been measured. Both gases were at room temperature and a pressure of about 60 atmospheres.

Several corrections have been applied to the observed intensities. Pressure and temperature differences, and pile power fluctuations need no elaborating. A volume correction arises from the variation of gas scattering volume with angle.

Multiple scattering, within the gas and from the wall, has been treated approximately (see Appendix), and finally, the background has been broken into its fast and slow neutron components and each considered separately.

The experimental points so obtained for CO_2 and O_2 are plotted in Figures 3 and 4 (pages 41 and 42) together with theoretical diffraction patterns for the same molecules. The calculated patterns are based on classical interference theory, and are similar in form to X-ray diffraction curves before the atomic form factor is introduced. Small corrections have been applied for a Doppler change in the neutron de Broglie wavelength due to the thermal motion of the gas molecules, and for a change of coordinates to the laboratory system. The greatest weakness of the calculation is that no account is taken of inelastic scattering, for the neutron energy (0.07 e.v.) is sufficient to excite many rotational transitions.

Three significant observations may be made from Figures 3 and 4. Firstly, both gases show good angular correlation between experimental points and the calculated curves. Secondly, oxygen also shows a good intensity correlation, though there is some deviation. Thirdly, carbon dioxide shows a fair intensity correlation only, the intensity being low at small angles. The angular correlation confirms within experimental error the accepted internuclear distances for the molecules. The small deviations of oxygen are likely due to experimental errors, but the large low angle deviation of carbon dioxide is most probably intermolecular interference from a vapour near its liquid phase.

2. INTRODUCTION

(a) History

(i) X-Ray and Electron Diffraction

In 1929 Debye, Bewilogua and Ehrhardt (1) first diffracted X-rays from a gas. Debye had shown theoretically in 1915 that an interference pattern was to be expected from the interatomic regularity in a single molecule, though the molecules themselves were randomly oriented and positioned in space (2). In addition diffraction patterns had been observed from crystals and liquids, which, analysis suggested, were in part due to intramolecular rather intermolecular interference. However the analysis was not easy in theory or in practice with bound molecules. For this reason it was hoped that coherent scattering from the unbound molecules of a gas might offer a better method for studying molecular structure.

Debye, et al., first used CCl_4 in the vapour state for their scattering material. X-ray scattering is a function of atomic number, and the sharp pattern from the regular tetrahedron of Cl atoms masks the C-Cl pattern, to give a very simple picture. The scattered rays were detected with a photographic film, and the gas chamber was so designed that the film could record only scattering from the gas itself and not from the metal walls. The pattern obtained with the 1.54 Å $K\alpha$ line from a copper target showed clearly an interference maximum at $34^{\circ} \pm 10$ percent. This gave 3.3Å as the

Cl-Cl spacing in the CCl_4 molecule and confirmed an earlier estimate from crystal diffraction of 1.72Å as the radius of the Cl^- ion. Many different molecules were soon investigated by Debye and his collaborators giving interatomic spacings for the molecules of a new order of accuracy (3).

In the following year Mark and Weirl successfully diffracted electrons by the free molecules of a gas (4). Again, CCl_4 was tried initially. They used a 30 kilovolt beam for which $\lambda = 0.071$Å, and found a first maximum at 1.6° and consequently a Cl-Cl spacing of 3.2Å. Within a year they had investigated many more gases and determined their interatomic distances and in some cases their molecular structure, with precision (5).

The results from this new field of physics were of primary interest to two groups: the physical chemist and the theoretical physicist. For, information given by X-ray and electron diffraction from simple molecules helped establish the present quantum-mechanical concept of the atom; and with an exact knowledge of the scattering power of the atom, it was possible to study complex molecular structure. The technique has become, together with molecular spectroscopy in the case of simple molecules, the basis for most of our present knowledge of interatomic bond lengths in gas molecules (6).

(ii) Neutron Diffraction

Evidence that slow neutrons are Bragg-reflected by a crystal was first obtained in 1936 by Mitchell and Powers (7), with a Rn-Be source and a set of Mg O crystals. The serious study of neutron diffraction by crystals, however, dates from the inception of the chain reacting pile. In 1944 Zinn first reported on measurements made with the neutron crystal spectrometer at the Argonne Laboratory (8), and this was followed closely by the results of a wide investigation at the same laboratory.

No work has been published however, on measurements of neutrons diffracted by gas molecules, and it is believed that the work herein reported is the first to be done in this field.

Fermi and Marshall (9) have measured the total cross section of a number of gases (CO_2, N_2O, O_2, N_2, CF_4 and H_2) for very slow neutrons, and found them, in most instances, to be in good agreement with the scattering cross sections calculated from classical interference theory. Since, for the energy of neutrons employed, these cross sections were substantially greater than the sums of the individual cross sections of the constituent atoms of the molecules, the experiment constituted excellent evidence for the diffraction of neutrons by a gas.

The present experiment was undertaken to verify, by an actual measurement of the angular dependence of the scattered beam, that monokinetic slow neutrons scattered by a gas do give a diffraction pattern. An improvement of the technique, it was hoped, would give useful information on gas molecular structure, and in particular, on the interaction between neutrons and nuclei.

(b) Theory

The same theory underlies the scattering by a gas target of a beam of homogeneous X-rays, electrons, or neutrons. When the wavelength of the quanta, or the de Broglie wavelength of the electrons or neutrons, is comparable to the internuclear distances of the molecule, there is coherence between the scattered waves from the individual atoms, and a diffraction pattern for the molecule as a whole. This pattern averaged over all the molecules of the gas gives a scattering pattern not isotropic as might be expected, but with interference maxima and minima characteristic of the structure of the scattering molecule and of the wavelength of the scattered beam. If the molecule has n atoms and each atom is assumed to scatter isotropically with equal phase change and amplitude, then the intensity of scattered beam $I(\theta)$ can easily be shown to be (10):

$$I(\theta) = \sum_{i=1}^{n} \sum_{j=1}^{n} \frac{\sin \chi_{ij}}{\chi_{ij}} \quad \text{where} \quad \chi_{ij} = 4\pi \ell_{ij} \frac{\sin \frac{\theta}{2}}{\lambda} \tag{1}$$

and

ℓ_{ij} is distance between i^{th} and j^{th} atoms

θ is angle between incident and scattered beams

λ is wavelength of scattered beam

In the above simplified picture, beams of quanta, electrons or neutrons behave identically since the atomic scattering centres are assumed to be points, scattering with equal phase change and amplitude, and with spherical symmetry. This however is not the case. In addition, only elastic scattering has been considered, whereas in practice, energy may be gained or lost by the beam in the scattering process. Equation (1) must be modified therefore to the more general form of equation (2) where the scattered beam is considered to have a coherent component and an incoherent component. Thus:

$$I(\theta) = \sum_{i\,1}^{n} \sum_{j\,1}^{n} \psi_i \psi_j \frac{\sin \chi_{ij}}{\chi_{ij}} + \xi \qquad (2)$$

where ψ_i and ψ_j are the "atomic scattering powers" of the i^{th} and j^{th} atoms, and ξ is the incoherent scattering term. Both ψ and ξ depend on the nature of the incident beam, whether X-ray, electron, or neutron, and are, in general, functions of the scattering angle θ. This dependence is shown qualitatively in Table 1.

It can be seen from Table I that two difficulties may lie in the way of a satisfactory theoretical determination of a diffraction pattern for neutrons scattered by a gas.

TABLE 1

	X-Rays (10)	Electrons (10)	Neutrons (9)
ψ	Scattering is from orbit electrons. Value obtained theoretically (by integration over probability function of orbit electrons). Magnitude approx. proportional to atomic number; decreases slightly with increasing scattering angle. Sign always positive. Function modified slightly by thermal motion of molecule (variation in inter-atomic distances).	Scattering is from nucleus, screened by orbit electrons. Value obtained theoretically. Magnitude approx. proportional to atomic number minus a screening factor; decreases rapidly ($1/\sin^4\theta/2$) with increasing scattering angle (θ). Sign always positive. Function modified slightly by thermal motion of molecule (variation in inter-atomic distances).	Scattering is from nucleus. Value obtained empirically. Magnitude erratic property of nuclide and relative spin of neutron and nucleus (parallel or anti-parallel); approx. independent of scattering angle. Sign erratically positive or negative. Function modified slightly by thermal motion of molecule (variation in inter-atomic distances, and neutron wave-length).
ξ	This function arises from the inelastic scattering processes and cannot be evaluated by the semi-classical methods used for elastic scattering. In the correct quantum-mechanical treatment both processes are considered as one problem and a detailed calculation of all possible transitions is made.		

Firstly, the amplitude and phase of the wave scattered from a given nuclide is, in general, not known. And secondly, a detailed calculation of all the rotational states involved is not in general practical. In special cases however these limitations either do not exist or are much less serious. For example, when a nucleus is that of a single isotope with zero spin, the atomic scattering power (ψ) is simply the square root of the nuclear cross section for that element. There may still be ambiguity in the sign of ψ but for many elements that too is known (9). A second simplification occurs at low temperatures, where sufficiently few rotational states may be involved that it is practical to calculate the inelastic component of scattering. This applies especially to light elements.

3. EXPERIMENTAL PROCEDURE

(a) Method I

Methane (CH_4) was chosen as the initial target. Not only has hydrogen a much larger cross section than any other element - and the problem of intensity was the first consideration - but its bond length is accurately known for only a few molecules, and the experiment should have given, if successful, its length for methane. The molecule CH_4 like CCl_4 is a regular tetrahedron, so the pattern was expected to give the strong maxima and minima characteristic of n-fold regularity. It was apparent at this time that the proton spin would likely introduce some incoherent scattering, and there was theoretical (11) and some experimental (9) evidence that it might be large. But until the incoherent scattering was later measured directly by Shull and Wollan (12) the diffraction experiment with methane appeared justified.

The apparatus was simple. The gas sample was placed directly in the neutron beam from an experimental hole in the Chalk River pile. Indium foils simultaneously selected and detected a monokinetic group of neutrons, for the 1.44 e.v. resonance rises to a peak of 26,000 barns and is less than 0.1 e.v. wide at half maximum value. The gas chamber was a heavy rotatable ground steel joint with two 0.006" aluminium windows. Secured to this joint were two cadmium and indium lined rectangular collimators for incident and scattered beams.

The indium foils were found to have a substantial background count from fast neutrons in spite of heavy shielding. This was overcome by using pairs of very thin (0.001") detector foils separated and backed by two thicker (0.005") foils of the same material. The difference of the two counts was taken as the resonance activation. More recently, Fermi and Marshall (13) have used a similar technique.

The foils were activated for two half lives (109 minutes), counted with a β-counter in the laboratory for two half lives, and were used repeatedly. Due to the complication of the difference technique of activation, foil calibration was difficult. Many tedious days of counting were required for adequate statistics. It was shown however, that the ratio of first minimum to first maximum departed from unity by less than 10%, confirming the earlier indications by Schwinger and Teller, and Fermi and Marshall, that CH_4 would scatter incoherently.

(b) Method II

(i) Procedure

By this time, the neutron flux from the pile was sufficient for the monokinetic beam from the neutron crystal spectrometer to give measurable intensities from a gas scatterer. The spectrometer equipment had been built by a Technical Physics group under Dr. D. G. Hurst, and it was only through his generosity in making it available that the author was able to perform the experiments described. The great advantage of the spectrometer over the foil technique was that only single energy neutrons were scattered from the target so intensities could be measured directly.

Consecutive scattering by crystal and gas, so diminished the neutron beam that the final intensity measured was only a few times background. Part of this background was fast neutrons from the primary beam of the spectrometer penetrating the counter shielding, but part too was fast neutrons, scattered from other experimental holes, penetrating the counter shielding. For this reason, most of the measurements were taken at night or during week-ends when other experimental activity was at a minimum. Since the experimental technique improved with time, the various runs were made in somewhat different ways, but in general the following procedure was adopted.

Throughout the experiment, the pile power was recorded continuously. Room temperature and gas pressure were in general read only at the beginning and end of a run, but if changes were suspected, also at intermediate intervals. It was assumed that the equilibrium gas temperature and ambient room temperature would be the same, since the maximum temperature variation of the air conditioned building is about ± 1°C. Initially the gas chamber and associated lines were evacuated and then filled to pressure from a high pressure gas cylinder. But later practice was to fill the vessel to pressure twice, allowing the first filling to flush out through a slightly loosened line connection, till a pressure of a few atmospheres only was reached.

Counting rates were measured at each scattering angle with the gas chamber filled and empty. In addition, at several angles, the fast neutron background was measured by covering the opening of the counter collimator with cadmium (and/or borated paraffin). For some runs the angle was varied continuously, for others intermittently. The counter H. T. voltage was monitored, but seldom altered as the regulation was very good. The scaler was operated with the scale-of-ten setting for all scattering measurements.

The neutron wavelength (λ), the scattering crystal lattice spacing (d), and the Bragg relationship ($n\lambda = 2d \sin \frac{\theta}{2}$) determined the spectrometer angle. Setting-up procedure then included crystal alignment for maximum beam intensity, and visual alignment at zero scattering angle of crystal, collimator, gas chamber, collimator and counter. For the scattering measurements, two geometries were employed. The first utilized two rectangular cadmium irises at the gas chamber, defining both incident and scattered beam; the second only one iris, for the incident beam. Since the iron walls at the chamber have a body-centred cubic crystal structure, the minimum scattering angle (except for a slight incoherent component) is twice the Bragg angle for the 1,1,0 planes, or approximately 32°. In the double iris geometry therefore the counter was exposed to iron which was in the neutron beam only at the non-scattering angles, i.e. below 29° for the particular dimensions of chamber and irises chosen. The double iris geometry was therefore used for the full sweep of scattering angles: 5° to 90°.

The single iris geometry however was used only for the smaller scattering angles, where there was low intensity from the walls. At the larger angles the scattered intensity from the walls was found to be many times that from the gas.

Two other measurements were made in addition to the scattering measurements. With neutron intensities reduced by a boron absorber in the main pile beam, the width of the mono-kinetic beam scattered from the crystal was measured. And as a check on the methods and constants used in analysing results, transmission measurements were made of the scattering chamber and gases. For this the scattering angle was set to zero, and two fine circular cadmium irises reduced sufficiently the beam intensity for counting losses to be negligible. In addition, an attempt was made to obtain one absolute calibration point by measuring the scattering at one angle from a gas known to scatter with spherical symmetry and to have a negligible absorption cross section. Helium was used. The measurements failed, however, for the gas was not of sufficient purity. A mass spectrometer analysis, performed by the pile control laboratory at Chalk River showed a hydrogen content greater than 0.7 percent. Unfortunately, because the scattering power of hydrogen is far greater than helium, the precision of the measurement did not allow a correction to be made for this impurity.

(ii) Apparatus

Figure 1 and photographs 1 - 3 show the experimental arrangement of pile, crystal spectrometer, collimators, gas chamber and counter. Neutrons from the high flux heavy water pile at Chalk River emerge from the collimator of one of the 4" experimental holes: a steel plug 81" long with a rectangular hole 1/2" wide by 1" high cut down its length. This beam is then Bragg-scattered in transmission from the planes (1,0,0) of a NaCl crystal, 1-1/16" wide by 1-7/8" high by 7/64" thick and placed 24" from the pile face. The unscattered portion is absorbed in a neutron catcher; a wooden box lined with cadmium, powdered boric acid, and paraffin, and with a 1/2" thick powdered boron absorber over its mouth. The diffracted portion passes down the 1/2" wide by 1" high channel of a steel collimator 1-9/16" x 4-1/4" x 19", striking the steel gas chamber 29.5" from the crystal, centre to centre. This collimator and the gas chamber are mounted on an arm carried by a Bofors gun turntable. On the same turntable and free to rotate coaxially is the crystal. The angular setting of both crystal and arm determine the neutron energy. (Both were fixed throughout the experiment since the energy remained unchanged). A second arm pivoted directly below the gas chamber, and coaxial with it, carries a further collimator and the counter and counter shield. This shield consists of three aluminium cylinders, 11", 5" and 2-3/4" in diameter and 40", 37" and 36" long respectively, containing an outer layer of paraffin and an inner layer of B_4C.

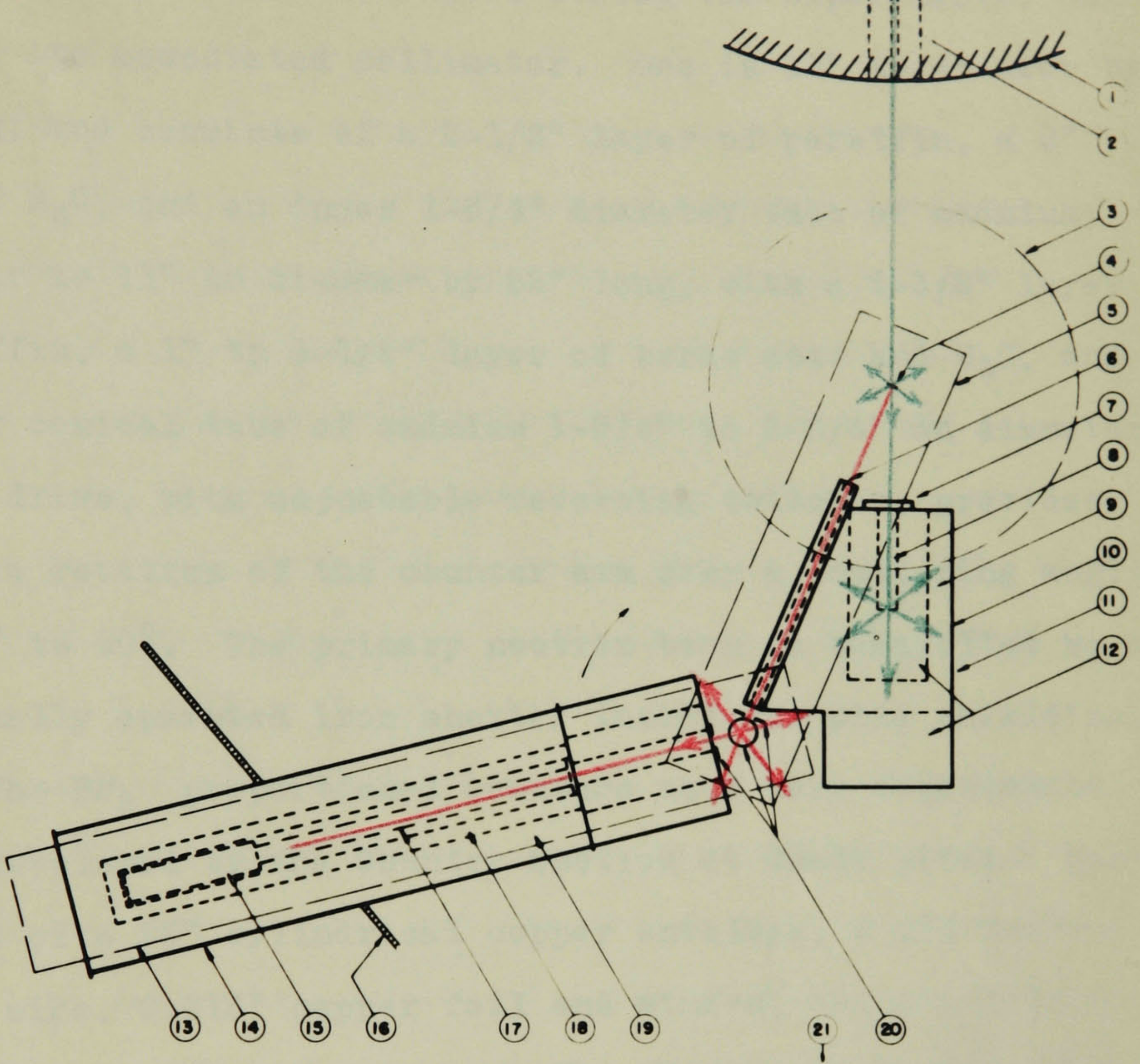

①	PILE SHIELD
②	STEEL COLLIMATOR
③	BOFORS TURNTABLE
④	CRYSTAL
⑤	TURNTABLE ARM
⑥	STEEL COLLIMATOR
⑦	BORON ABSORBER
⑧	AIR SHAFT
⑨	BORIC ACID POWDER
⑩	CADMIUM LINING
⑪	NEUTRON CATCHER
⑫	PARAFFIN
⑬	COUNTER ARM
⑭	COUNTER SHIELD
⑮	PREAMPLIFIER
⑯	DRIVE SCREW
⑰	COUNTER
⑱	BORON CARBIDE
⑲	PARAFFIN
⑳	GAS CHAMBER & CADMIUM IRISES
(21)	γ - SHIELD

—	NEUTRON BEAM — ALL ENERGIES
—	MONOKINETIC NEUTRON BEAM

Figure 1 - Experimental Arrangement of Crystal Spectrometer and Gas Scattering Apparatus

Two different counters were used during the experiments, and each had its associated collimator. One is 11" in diameter by 11" long, and consists of a 2-1/2" layer of paraffin, a 2" layer of B_4C, and an inner 1-3/4" diameter tube of cadmium; the other is 11" in diameter by 22" long, with a 2-1/2" layer of paraffin, a 1" to 1-1/2" layer of boric acid and B_4C, and an inner conical tube of cadmium 1-3/4" to 2-3/4" in diameter. A motor drive, with adjustable reversing switches, provides automatic rotation of the counter arm over a scattering angle range 0^o to 90^o. The primary neutron beam is controlled by an electrically operated iron shutter inside the pile shielding.

The BF_3 proportional counters used were experimental models developed by the Counter Section at Chalk River. Each consists of a 25" cylindrical copper envelope, 2 mil central tunsten wire, 0.010" copper foil end window, and about 68 cm. of mercury pure BF_3 atmosphere. The first is 1-1/4" in diameter, the second 2-5/16" in diameter. Natural boron is used for the first, B_{10} for the second; giving calculated efficiencies of 47 percent and 95 percent respectively for 0.07 e.v. neutrons traversing the 55 cm. active length. The bias and H.T. curves of the two counters determined the operating voltages to be 2700 volts and 3300 volts respectively. With the discriminator bias settings used, counter 1 showed a negligible H.T. plateau, but counter 2 was flat for 200 volts. Counter 1 was measurably insensitive to γ's, but counter 2 was not checked.

Fig. 2 is a block diagram of the associated electrical circuits for the spectrometer. The pile power monitor is an ion chamber (first column) in the pile north thermal column. It feeds a Brown converter and a.c. feedback amplifier (N.R.C. design) which in turn feeds an Esterline-Angus recording ammeter. With normal scale limits of ± 25 percent pile power, the pile power can be read to better than 0.5 percent. In the counter chain (third column) are: laboratory built, cathode-follower pre-amplifier; N.R.C. power supply, type 200; Atomic Instruments linear amplifier, model 204-C; N.R.C. counting rate meter, G.P.MK.1; T.R.E. scaler, type 200; and finally two Esterline-Angus recording meters, a single pen, and a ten-pen. The former meter records from the counting rate meter: integrated counting rate; and the latter meter records from the scaler: individual counts of ten, and from the motor control chassis: time pulses (minutes), revolutions (every twenty) and sense of the counter arm drive screw. With the exception of the pre-amplifier which is behind the counter and within the counter shield (see Fig. 1), and the converter - a.c. amplifier, which is near the ion chamber, the chassis and meters are accommodated in relay racks adjacent to the spectrometer (see Photograph 3).

The gas chamber (see Photograph 4) is a mild steel cylinder 2.000 ± .001" i.d., 2.160 ± .001" o.d., by 3" long, closed at top and bottom with 3/4" and 1/4" thick end walls.

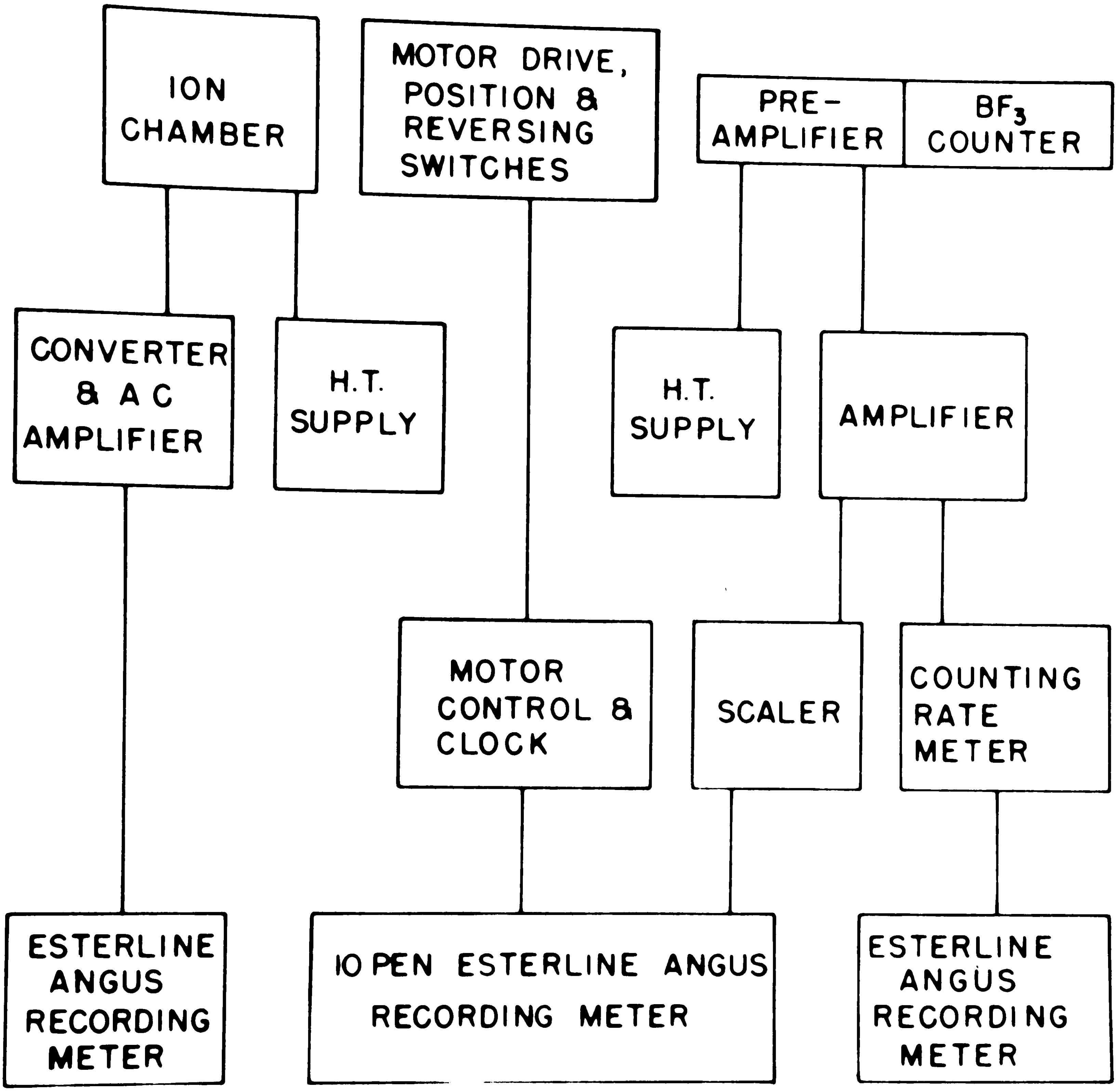

FIG.2 - BLOCK DIAGRAM OF ELECTRONIC CIRCUITS FOR NEUTRON CRYSTAL SPECTROMETER

It is designed for gas at 1000 p.s.i. with a safety factor of four. A special tee pipe fitting at the top secures the gas supply valve and pressure gauge to the chamber. Beyond this valve is a 2" length of 3/16" i.d. pipe terminating in a standard high pressure gas cylinder connector. Two pressure gauges were used: a 0-3000 p.s.i. Airco (Air Reduction Sales Co., New York) with 100 p.s.i. subdivisions, and a 0-1000 p.s.i. Ashcroft Laboratory Test Gauge with 5 p.s.i. subdivisions. Both were calibrated against an Ashcroft Standard Gauge Tester by an operations test group at Chalk River. The beam irises are 1.00" by 0.50" inside, and are cut from 1/32" thick cadmium sheet. The first is mounted on a slotted brass plate to be 1-7/16" from the centre of the gas chamber; the second, used only in the double slit geometry, is secured to the front face of the counter collimator.

4. EXPERIMENTAL RESULTS

(a) Carbon Dioxide Scattering

Carbon dioxide was chosen as the initial target for measurements with the neutron spectrometer. The incoherent pattern of methane as measured with indium foils, was believed due to spin dependence in the n-p interaction. However since carbon is predominantly C^{12} and oxygen predominantly O^{16} both of which have zero spin, the scattering amplitude and phase change for each element must be single valued, and since the phase of scattered wave is the same for carbon and oxygen (9) the resultant pattern should be coherent. In addition, the diffraction pattern for CO_2 as given by equation (2) is more pronounced than that for a simple diatomic molecule; and its cross section is larger (partly due to there being three atoms, and partly to its abnormally large density at high pressure).

The target gas was taken directly from a high pressure container supplied by the Liquid Carbonic Company. Five runs were made, where by a run we mean a sequence of measurements with the chamber filled and empty. The spectrometer was set to a Bragg angle of 11°, to give monokinetic neutrons of 0.070 e.v. energy from the (1,0,0) planes of the NaCl crystal (lattice spacing 5.628 Å.). Counter 1, 1-1/4" in diameter, was used for all runs. The measured monokinetic beam width (half intensity) was 2.5° for both double and single slit geometries. Details of the experimental arrangement for each of the five runs are summarized in Table 2. No temperature measurements were made for runs 1, 2 and 3; the pressure drop during runs 2, 3 and 5 was due to a leaking valve. Table 3 gives the scattered beam intensities, gas pressures, temperature, and relative pile powers as a function of scattering angle, taken during the five runs. Gas pressures, room temperatures, and pile powers shown are averages taken over the portion of the run considered for each angle.

TABLE 2

Run	Running Time	Mode of Operation	Gas pressures and temperature	Pressure Gauge	Geometry
1	32 hrs.	angle varied continuously from 22° to 84° - gas in for 1/2 cycle sweep, out for 1/2 cycle	800 p.s.i. and 0 p.s.i.	Airco	double iris - window of counter 13-1/4" from centre of gas chamber
2	35 hrs.	angle varied continuously from 8° to 31° gas in for 2 cycles, out for 1-1/2 cycles	770 to 750 p.s.i. and 0 p.s.i.	"	"
3	64 hrs.	angle fixed at 42°, 62°, 85°	750 to 720 p.s.i. and 0 p.s.i.	"	"
4	23 hrs.	angle fixed at 5°, 10°, 17°	818 to 825 p.s.i., 21.5° to 22.0°C. and 15 p.s.i.	Ashcroft	single iris - window of counter 21-1/8" from centre of gas chamber
5	31 hrs.	angle fixed at 26°, 40°	784 to 591 p.s.i., 22.4° to 23.6°C. and 15 p.s.i.	"	

ANGLE (DEGREES)	GAS + TOTAL BACKGROUND				GAS PRESSURE	TOTAL BACKGROUND			FAST NEUTRON BACKGROUND [3, 4]
	GAS PRESSURE & TEMPERATURE [2]	MEASURED VALUE [2 3]	RELATING PILE POWER [2]	CORRECTED FOR PILE POWER		MEASURED VALUE [2 3]	RELATING PILE POWER [2]	CORRECTED FOR PILE POWER	
5.0′	818 PSI 21.5°C	131.7 ± 1.0	1.023	128.7 ± 1.0	15 PSI	59.3 ± 0.7	1.032	57.5 ± 0.7	14 ± 1
9.5	760 PSI	92.6 ± 1.2	1.033	89.7 ± 1.2	0	60.0 ± 0.8	1.049	57.2 ± 0.8	(8)
10.0′	828 PSI 22.4°C	105.3 ± 0.6	1.021	103.1 ± 0.6	15	54.0 ± 0.7	1.027	52.5 ± 0.7	7 ± 2
12.7	760 PSI	65.3 ± 0.7	1.033	63.2 ± 0.7	0	34.6 ± 0.6	1.045	33.1 ± 0.6	(6)
15.9	760 PSI	56.5 ± 0.6	1.034	54.6 ± 0.6	0	27.1 ± 0.5	1.046	25.9 ± 0.5	(6)
17.0′	832 PSI 22.7°C	101.5 ± 0.7	1.025	99.1 ± 0.7	15	52.3 ± 0.3	1.018	51.4 ± 0.3	(6)
19.1	760 PSI	48.5 ± 0.5	1.035	46.8 ± 0.5	0	24.3 ± 0.5	1.048	23.2 ± 0.5	(6)
22.3	760 PSI	41.1 ± 0.6	1.040	39.5 ± 0.6	0	20.2 ± 0.4	1.050	19.2 ± 0.4	(6)
24.4	800 PSI	40.4 ± 0.6	1.026	39.4 ± 0.6	0	19.6 ± 0.4	1.040	18.9 ± 0.4	(6)
25.6	760 PSI	36.9 ± 0.7	1.036	35.6 ± 0.7	0	19.3 ± 0.4	1.053	18.3 ± 0.4	(6)
26.0′	757 PSI 22.4°C	80.4 ± 0.6	1.024	78.5 ± 0.6	15	48.8 ± 0.3	1.031	47.3 ± 0.3	(6)
28.6	800 PSI	39.3 ± 0.9	1.027	38.3 ± 0.9	0	24.1 ± 0.5	1.049	23.0 ± 0.5	(5)
29.0	760 PSI	45.6 ± 0.5	1.046	43.6 ± 0.5	0	31.8 ± 0.4	1.056	30.1 ± 0.4	(5)
35.6	800 PSI	32.7 ± 0.9	1.039	31.4 ± 0.9	0	22.8 ± 0.7	1.062	21.5 ± 0.7	(5)
40.0′	660 PSI 23°C	64.4 ± 0.3	1.037	62.1 ± 0.3	15	44.9 ± 0.3	1.029	43.6 ± 0.3	(5)
40.3	800 PSI	21.1 ± 0.6	1.037	20.4 ± 0.6	0	10.2 ± 0.4	1.063	9.6 ± 0.4	(5)
42.0	745 PSI	18.0 ± 0.2	1.038	17.3 ± 0.2	0	8.3 ± 0.1	1.023	8.1 ± 0.1	(5)
45.8	800 PSI	19.2 ± 0.5	1.040	18.5 ± 0.5	0	7.8 ± 0.4	1.056	7.4 ± 0.4	(5)
51.6	800 PSI	18.1 ± 0.5	1.039	17.4 ± 0.5	0	7.5 ± 0.4	1.063	7.1 ± 0.4	5.0 ± 0.4
57.9	800 PSI	18.9 ± 0.5	1.038	18.2 ± 0.5	0	7.0 ± 0.4	1.055	6.8 ± 0.4	(5)
62.0	735 PSI	16.8 ± 0.2	1.031	16.3 ± 0.2	0	6.2 ± 0.1	1.030	6.05 ± 0.1	(5)
64.6	800 PSI	18.9 ± 0.4	1.035	18.3 ± 0.4	0	6.5 ± 0.3	1.055	6.2 ± 0.3	(5)
71.9	800 PSI	17.0 ± 0.4	1.033	16.5 ± 0.3	0	6.3 ± 0.3	1.046	6.0 ± 0.3	(5)
80.0	800 PSI	16.4 ± 0.3	1.031	15.9 ± 0.3	0	6.3 ± 0.3	1.031	6.1 ± 0.3	(5)
85.0	725 PSI	14.2 ± 0.2	1.031	13.8 ± 0.2	0	6.1 ± 0.1	1.035	5.9 ± 0.1	(5)

NOTES

(1) SINGLE SLIT GEOMETRY, OTHERWISE DOUBLE SLIT (SEE TEXT)
(2) AVERAGE VALUE
(3) WITH STANDARD DEVIATION
(4) THROUGH COUNTER SHIELD (GAS CHAMBER REPLACED WITH CADMIUM)
MOST PROBABLE VALUES (BRACKETED) ARE ESTIMATES BASED ON
THE FEW MEASURED VALUES (UNBRACKETED)

TABLE 3 - EXPERIMENTAL INTENSITIES OF SCATTERED NEUTRON BEAMS (COUNTS/MIN) FOR CO_2 GAS AS A FUNCTION OF SCATTERING ANGLE

(b) Oxygen Scattering

The second target gas, oxygen, was selected in order to investigate the large deviation found in the carbon dioxide pattern. It was thought the low intensity at small angles might be due to CO_2 at 50 atmospheres and room temperature being near the liquid phase. Since O_2 under these same conditions was far from the liquid phase this hypothesis could be checked. The gas of course has the same desirable isotopic and spin characteristics as CO_2, but being diatomic has not as large a cross section nor quite as pronounced an interference pattern.

Electrolytic oxygen of purity better than 99.6 percent was used from a tank supplied by the Dominion Oxygen Company. Three runs were made, and as before, the neutron energy was set at 0.070 e.v. An improved counting rate was obtained with counter 2 due to its larger diameter (2-5/16") and the B_{10} enriched filling. Double irises, and a distance from counter window to gas chamber centre of 25" combined to give a measured beam width of 3.6°. Pressures were read with the Ashcroft Laboratory Test Gauge. All scattered intensities were measured with the counting arm fixed at a given angle rather than being rotated continuously. Other relevant experimental details for each run are given in Table 4. Table 5 gives the scattered beam intensities, gas pressures, ambient temperature, and relative pile powers as a function of scattering angle, taken during the three runs. As before, the pile power values are averages for the portion of the run concerned.

TABLE 4

Run	Running Time	Angles	Gas Pressures	Temperatures
1	39 hrs.	10°, 15°, 20°, 28°, 36°	953 p.s.i. to 944 p.s.i. and 22 p.s.i.	23.3°C. 21.3°C.
2	16 hrs.	45°, 55°, 65° 10°	920 p.s.i. to 919 p.s.i. and 19 p.s.i.	22.4°C. 21.7°C.
3	10 hrs.	75°, 85°, 15°	903 p.s.i. to 904 p.s.i. and 17 p.s.i.	21.5°C. 21.7°C.

(c) Transmission Measurements

The attenuation of the 0.07 e.v. neutron beam by iron (the gas chamber) and by carbon dioxide and oxygen gases at a number of pressures was measured. For this, the scattering angle was set to zero, and the monokinetic spectrometer beam was stopped down by two fine cadmium diaphragms. Counting rates were then taken with and without the given attenuator in the beam. The spectrometer beam however, has a small fast neutron component incoherently scattered from the crystal. To sort out this fast (and therefore epi-cadmium) component, all measurements were repeated with a cadmium absorber over the counter. Results for all runs are given in Table 6. The rates have been corrected for any slight differences in pile power, before entry in the table.

ANGLE (DEGREES)	GAS + TOTAL BACKGROUND				TOTAL BACKGROUND				FAST NEUTRON BACKGROUND [2,3]
	GAS PRESSURE & TEMPERATURE	MEASURED VALUE [1,2]	RELATING PILE POWER [1]	CORRECTED FOR PILE POWER	GAS PRESSURE	MEASURED VALUE [1,2]	RELATING PILE POWER [1]	CORRECTED FOR PILE POWER	
10	953 PSI 23.3°C	267.8 ±2.1	1.013	264.3 ±2.1	22 PSI	139.0 ±1.7	0.977	142.2 ±1.7	10±2 (10)
10	919 PSI 21.7°C	255.5 ±3.6	0.979	260.9 ±3.6	19	142.3 ±3.3	0.979	145.3 ±3.3	(10)
15	953 PSI 23.3°C	214.5 ±1.6	1.008	212.9 ±1.6	22	105.4 ±1.2	0.986	107.0 ±1.2	(11)
15	904 PSI 21.7°C	210.8 ±2.4	0.984	214.1 ±2.4	16	108.5 ±1.6	0.984	110.2 ±1.6	(11)
20	953 PSI 23.3°C	160.2 ±1.6	0.990	161.8 ±1.6	22	86.9 ±1.2	0.996	87.2 ±1.2	12±2 (12)
28	953 PSI 23.3°C	114.8 ±0.6	1.003	114.5 ±0.6	22	70.8 ±0.4	0.993	71.4 ±0.4	(13)
36	944 PSI 21.3°C	70.2 ±0.4	0.983	71.4 ±0.4	22	39.1 ±0.2	0.995	39.3 ±0.2	11±2 (14)
45	920 PSI 22.4°C	67.1 ±1.0	1.000	67.1 ±1.0	19	38.0 ±0.9	0.979	38.8 ±0.9	14±2 (16)
55	920 PSI 22.3°C	64.3 ±1.2	1.000	64.3 ±1.2	19			38.3 ±1.1	20±2 (18)
65	919 PSI 21.7°C	59.9 0.4	0.997	60.1 0.4	19	31.0 0.3	0.981	31.6 0.3	18±2 (20)
75	903 PSI 21.5°C	56.9 ±0.5	0.986	57.7 ±0.5	17	34.4 ±0.4	0.985	34.9 ±0.4	25±2 (22)
85	903 PSI 21.5°C	57.2 ±0.9	0.983	58.2 ±0.9	17	38.7 ±1.0	0.987	39.2 ±1.0	25±2 (24)

NOTES

(1) AVERAGE VALUE

(2) WITH STANDARD DEVIATION

(3) THROUGH COUNTER SHIELD (GAS CHAMBER REPLACED WITH CADMIUM)
MOST PROBABLE VALUES (BRACKETED), TAKEN FROM PLOT OF
MEASURED VALUES (UNBRACKETED), ARE USED FOR SUBSEQUENT CALCULATIONS

TABLE 5 – EXPERIMENTAL INTENSITIES OF SCATTERED NEUTRON BEAMS (COUNTS/MIN) FOR O_2 GAS AS A FUNCTION OF SCATTERING ANGLE

TABLE 6

Run	Attenuator	Gas Pressure and temperature	Counts/min. without cadmium	Counts/min. with cadmium
1	gas chamber + O_2	901 p.s.i. at 23.0°C.	13,120 ± 50	411 ± 8
2	" " "	614 p.s.i. at 23.1°C.	13,410 ± 40	406 ± 10
3	" " "	314 p.s.i. at 23.1°C.	13,630 ± 50	405 ± 10
4	" " "	17 p.s.i. at 23.1°C.	13,890 ± 50	420 ± 10
5.	no chamber	-	21,410 ± 70	578 ± 11
6	gas chamber + CO_2	778 p.s.i. at 23.2°C.	12,230 ± 40	363 ± 9
7	" " "	710 p.s.i. at 23.3°C.	12,410 ± 40	350 ± 13
8	" " "	353 p.s.i. at 23.3°C.	13,340 ± 50	407 ± 10
9	" " "	20 p.s.i. at 23.3°C.	13,830 ± 50	380 ± 10

5. CALCULATIONS

(a) Scattering Corrections

Several corrections must be applied to the measured neutron intensities to obtain the true angular dependence of scattering. They are described below, and applied to the carbon dioxide and oxygen results of Tables 3 and 5, in Tables 7 and 8.

(i) Pressure and temperature - In the pressure and temperature range of the experiment, oxygen satisfies the perfect gas law, and this equation has been used to obtain the density of the gas for the various conditions of temperature and pressure. Carbon dioxide however, has been measured in a region very close to its critical point, so that $pv \neq RT$. A better approximation, the Plank-Kuprianoff equation (14) does accurately fit our data and it has been used to obtain the various densities:

$$V = \frac{19.27T}{p} - \frac{.0825 + 1.225 \times 10^{-7} p}{\left(\frac{T}{100}\right)^{10/3}} \qquad (3)$$

where:

V is specific volume in meters/kg. (1/density)

p is pressure in kg./meters^2

T is temperature in degrees absolute

The density of gas in the background run was subtracted from the density of gas in the pressure run. All data were then corrected to an average standard condition, 775 p.s.i. and 22.3°C for CO_2, 910 p.s.i. and 22.3°C for O_2. Where no

ANGLE (DEGREES)	GAS CHAMBER BACKGROUND		GAS		VOLUME CORRECTION		NORMALIZED [5]	DOUBLE SCATTERING CORRECTION [4]	
	UNATTENUATED [2]	ATTENUATED BY GAS [3]	AT MEASURED PRESSURE & TEMPERATURE	AT 775 PSI 22.3°C [4]	RELATIVE VOLUME SCAT. GAS [4]	CORRECTED FOR GAS VOLUME		VALUE OF DOUBLE SCATTERING [6]	CORRECTED FOR DOUBLE SCATTERING
5.0′	43.5	37.4	77.3 ± 1.2	69.4	—	—	2.227	.212	2.015 ± .03
9.5	49.2	43.3	38.4 ± 1.4	40.0	3.338	11.97	1.520	.086	1.434 ± .05
10.0′	48.5	39.0	57.1 ± 0.9	50.7	—	—	1.628	.212	1.416 ± .02
12.7	27.1	23.8	33.4 ± 0.9	34.8	3.130	11.12	1.413	.085	1.328 ± .04
15.9	19.9	17.5	31.1 ± 0.8	32.4	2.922	11.10	1.411	.085	1.326 ± .03
17.0′	45.4	38.9	54.2 ± 0.8	48.1	—	—	1.544	.212	1.332 ± .02
19.1	17.2	15.1	25.7 ± 0.7	26.8	2.712	9.89	1.257	.085	1.172 ± .03
22.3	13.2	11.6	21.9 ± 0.7	22.8	2.503	9.11	1.157	.085	1.072 ± .03
24.4	12.9	11.2	22.2 ± 0.7	20.9	2.365	8.84	1.123	.085	1.038 ± .03
25.6	12.3	10.8	18.8 ± 0.8	19.6	2.288	8.56	1.087	.085	1.002 ± .04
26.0′	41.3	36.4	36.1 ± 0.7	38.4	—	—	1.233	212	1.021 ± .02
28.6	18.0	15.6	17.7 ± 1.0	16.7	2.092	7.99	1.014	084	0.930 ± .05
29.0	25.1	22.1	16.5 ± 0.6	17.2	2.063	8.34	1.059	084	0.975 ± .03
35.6	16.5	14.3	12.1 ± 1.1	11.4	1.718	6.64	0.844	084	0.760 ± .07
40.0′	38.6	35.0	22.1 ± 0.4	29.8	—	—	0.957	.212	0.745 ± .02
40.3	4.6	4.0	11.4 ± 0.7	10.7	1.547	6.91	0.877	084	0.793 ± .05
42.0	3.1	2.74	9.56 ± 0.2	10.32	1.493	6.91	0.877	085	0.792 ± .02
45.8	2.4	2.1	11.4 ± 0.6	10.7	1.395	7.67	0.974	085	0.889 ± .05
51.6	2.1	1.8	10.6 ± 0.6	10.0	1.276	7.84	0.996	086	0.910 ± .06
57.9	1.6	1.4	11.8 ± 0.6	11.1	1.180	9.40	1.193	.087	1.106 ± .06
62.0	1.05	0.93	10.37 ± 0.2	11.44	1.132	10.12	1.286	.089	1.197 ± .02
64.6	1.2	1.0	12.3 ± 0.5	11.6	1.108	10.47	1.330	.090	1.240 ± .05
71.9	1.0	0.9	10.6 ± 0.4	10.0	1.052	9.51	1.207	.092	1.115 ± .04
80.0	1.1	1.0	9.9 ± 0.4	9.3	1.015	9.17	1.164	.096	1.068 ± .04
85.0	0.9	0.8	8.0 ± 0.2	9.05	1.004	9.01	1.144	.099	1.045 ± .03

NOTES

(1) SINGLE SLIT GEOMETRY, OTHERWISE DOUBLE SLIT (SEE TEXT)

(2) TOTAL BACKGROUND MINUS FAST NEUTRON BACKGROUND

(3) SCATTERED BY CHAMBER WITH GAS AT ZERO OR ATMOSPHERIC PRESSURE, CORRECTED TO VALUE WITH GAS AT HIGH PRESSURE (SEE TEXT)

(4) SEE TEXT

(5) TO GIVE BEST FIT TO THEORETICAL CURVE AFTER CORRECTION FOR DOUBLE SCATTERING – SINGLE SLIT GEOMETRY X 0.321 – DOUBLE SLIT GEOMETRY X 0.127

(6) INTERPOLATED FROM VALUES CALCULATED IN APPENDIX

TABLE 7 – CORRECTED INTENSITIES OF SCATTERED NEUTRON BEAMS (COUNTS/ MIN) FOR CO_2 GAS AS A FUNCTION OF SCATTERING ANGLE

ANGLE (DEGREES)	GAS CHAMBER BACKGROUND		GAS		VOLUME CORRECTION		NORMALIZED [4]	DOUBLE SCATTERING CORRECTION [3]	
	UNATTENUATED [1]	ATTENUATED BY GAS [2]	AT MEASURED PRESSURE & TEMPERATURE	AT 910 PSI 22.3° C [3]	RELATIVE VOLUME SCAT GAS [3]	CORRECTED FOR GAS VOLUME		VALUE OF DOUBLE SCATTERING [5]	CORRECTED FOR DOUBLE SCATTERING
10	132.2	124.2	130.1 ± 2.7	127.8	3.306	38.65	1.837	.070	1.767 ± .04
10	135.3	127.2	123.7 ± 4.9	124.8	3.306	37.75	1.793	.070	1.723 ± .07
15	96.0	90.2	111.7 ± 2.0	109.7	2.979	36.83	1.750	.068	1.682 ± .03
15	99.2	93.3	109.8 ± 2.9	112.3	2.979	37.70	1.791	.068	1.723 ± .04
20	75.2	70.7	79.1 ± 2.0	77.6	2.653	29.25	1.390	.067	1.323 ± .03
28	58.4	54.9	46.6 ± 0.7	45.7	2.131	21.47	1.022	.066	.956 ± .015
36	25.3	23.8	33.6 ± 0.45	33.05	1.702	19.42	0.923	.065	.858 ± .01
45	22.8	21.4	29.7 ± 1.3	30.0	1.414	21.20	1.007	.064	.943 ± .04
55	20.3	19.1	27.2 ± 1.6	27.45	1.221	22.50	1.068	.065	1.003 ± .04
65	11.6	10.9	29.2 ± 0.5	29.47	1.103	26.73	1.269	.067	1.202 ± .02
75	12.9	12.1	23.6 ± 0.6	24.13	1.035	23.30	1.107	.070	1.037 ± .03
85	15.2	14.3	19.9 ± 1.3	20.35	1.004	20.27	0.964	.074	0.890 ± .06

NOTES

(1) TOTAL BACKGROUND MINUS FAST NEUTRON BACKGROUND

(2) SCATTERED BY CHAMBER WITH GAS AT APPROXIMATELY ATMOSPHERIC PRESSURE, CORRECTED TO VALUE WITH GAS AT HIGH PRESSURE X 0.960

(3) SEE TEXT

(4) TO GIVE BEST FIT TO THEORETICAL CURVE AFTER DOUBLE SCATTERING CORRECTION APPLIED X 0.475

(5) INTERPOLATED FROM VALUES CALCULATED IN APPENDIX

TABLE 8 – CORRECTED INTENSITIES OF SCATTERED NEUTRON BEAMS (COUNTS / MIN) FOR O_2 GAS AS A FUNCTION OF SCATTERING ANGLE

temperatures were taken, the standard temperature was assumed, and where the pressure during a run varied considerably (e.g. at 40^0, run 5, Table 2) the run was broken into intervals and each one calculated separately. This served in fact as a useful check on this correction.

(ii) Pile power - This is a direct correction to counting rate, and has already been done in Tables 3 and 5.

(iii) Scattering volume (see Fig. 1A, (b) and (c) page 57) With the single slit geometry, the counter "sees" the same volume of scattering gas independent of angle. With two irises however, the volume is a function of angle. It can be proven easily that for $\frac{1}{2}$" by 1" defining slits and a 2" i.d. gas chamber:

$$V = \pi \left(\frac{14.5^0 - \frac{\theta}{2}}{22.5^0} \right) + 2 \frac{\cos(14.5^0 - \frac{\theta}{2})}{\cos \frac{\theta}{2}} \qquad \text{for } 0^0 < \theta < 29^0$$

$$= \frac{1}{\sin \theta} \qquad \text{for } 29^0 < \theta < 90^0 \qquad (4)$$

where:

V is the volume of scattering gas in inches^3

θ is the angle between incident and scattered beams in degrees.

(iv) Multiple scattering - This effect arises from the wall of the gas chamber and the gas itself. Its magnitude is not known rigorously, for the calculation, though possible, is not easy. A multiple integration involving explicit functions for the angular distribution of both wall and gas is required, for double, triple, etc. scattering in turn. Approximate solutions have been worked out however (see the Appendix) by considering only double scattering, and by assuming the gas to scatter isotropically, the wall to scatter not at all up to 30^{o}, and isotropically beyond 30^{o}. Numerical calculations are given of the ratio, double to single scattering, for the two geometries of our experiment. They show that with the approximations used, this ratio is very nearly independent of angle for both the single and double slit geometry. The scattering powers of the wall and the two gases are based on equation (5) and Table 9, column 5 (see next section). Since single scattering is assumed spherically symmetrical and is normalized to unity, the double to single scattering ratios represent the absolute values of multiple scattering. As the final correction they are therefore subtracted directly.

(v) Attenuation - Attenuation of the incident and scattered beams by walls and gas is appreciable, but since the path length is nearly independent of scattering angle, it has been neglected. Were the gas density to have differed greatly between runs, a correction would have been applied.

(vi) Background - The background run (vacuum or atmospheric) cannot be subtracted simply from the high pressure run to give the true gas scattered part. Why not? Because that fraction of the background, which is caused by the monokinetic beam scattering from the vessel walls is unattenuated in the background run, but attenuated by the gas in the pressure run.

it must therefore be decreased accordingly before subtraction. This may be better understood by considering what makes up background. Roughly it may be divided into three parts. Firstly, there are fast neutrons from all directions reaching the counter by penetrating its shielding. This is the predominant portion at large angles. Secondly, fast neutrons in the monokinetic beam scatter from the chamber and pass up the counter collimator by penetrating the second cadmium iris. And finally, 0.07 e.v. neutrons scatter from the chamber. This is the predominant portion at small angles. As already described (see "Apparatus") most of the slow neutron scattering from the vessel walls is effectively blocked by the geometry of the system. Therefore what remains, from this source, is likely an incoherent component at small angles, and a wall-wall doubly scattered component at large angles.

The intensity of fast neutrons penetrating the counter shield was measured directly by replacing the gas chamber with a sheet of cadmium. Subtraction from the run with the vessel empty leaves the background of fast and slow neutrons scattered from the gas chamber. This remainder is then corrected for gas attenuation, without further background separation since the scattering cross sections of carbon and oxygen are very nearly constant from 0.07 e.v. to 100 Kev. (15). Gas attenuation is based on equation (5), with values of σ from Table 9, column 5.

(b) Transmission Measurements

In general a neutron beam is attenuated by absorption and scattering. Since for iron, oxygen and carbon the absorption cross section is very small (16) we may consider the attenuation as due to scattering.

Let X be the transmitted fraction of the beam. Then:

$$X = e^{-\frac{t\rho\sigma N}{A}} \qquad (5)$$

where t is thickness of scattering substance in cm.

ρ is density of scattering substance in gm./$cm.^3$

σ is molecular scattering cross section in $cms.^2$

A is atomic weight of scattering substance

N is Avagadro's number

Using equation (5) and the data from Table 6, experimental values for the molecular scattering cross section have been calculated. Equation (3) is used as before for the density of CO_2. The slow neutron transmission (X) is the ratio of counting rates with and without the scatterer in the beam, after the fast neutron component (column 5, Table 6) has been subtracted from the total (column 4, Table 6). The total thickness of iron is taken as 0.406 cm. and of gas 5.08 cm. These results are given in the first four columns of Table 9. In the fifth column, for comparison, is given the sum of the atomic scattering cross sections. For 0.07 e.v. neutrons, the atomic cross section of iron is 12.7 barns (10^{-24} $cm.^2$) of carbon is 4.7 barns, and of oxygen is 3.9 barns (15).

TABLE 9

Scattering substance	Density (ρ)	Slow neutron transmission (X)	Experimental molecular scattering cross section	Sum of scattering cross sections of constituent atoms
Fe	7.8	0.646 ± .003	12.7 ± 0.2	12.7 barns
CO_2	0.153	0.882 ± .004	11.7 ± 0.5	12.5 barns
	0.129	0.896 ± .004	12.2 ± 0.6	12.5 barns
	0.048	0.961 ± .005	12.1 ± 1.5	12.5 barns
O_2	0.079	0.945 ± .005	7.4 ± 0.7	7.8 barns
	0.053	0.966 ± .005	6.8 ± 1.0	7.8 barns
	0.026	0.984 ± .005	6.4 ± 1.8	7.8 barns

(c) Theoretical Curves

(i) Diffraction Patterns

Both CO_2 and O_2 very nearly satisfy the conditions: (a) constituent atoms are single isotopes, (b) nuclei have zero spin, (c) phase of scattered wave same for all atoms in molecule (9). Therefore we may write for the intensity (I) of the elastically scattered neutron beam:

Carbon Dioxide:

$$I = K_1\left(2\psi_1^2 + \psi_2^2 + 2\psi_1^2 \frac{\sin\left(\frac{4\pi \ell_1 \sin\frac{\theta}{2}}{\lambda}\right)}{\frac{4\pi \ell_1 \sin\frac{\theta}{2}}{\lambda}} + 4\psi_1\psi_2 \frac{\sin\left(\frac{4\pi \ell_2 \sin\frac{\theta}{2}}{\lambda}\right)}{\frac{4\pi \ell_2 \sin\frac{\theta}{2}}{\lambda}}\right) \qquad (6)$$

Oxygen:

$$I = K_2\left(2\psi_1^2 + 2\psi_1^2 \frac{\sin\left(\dfrac{4\pi \ell_1 \sin\frac{\theta}{2}}{\lambda}\right)}{\dfrac{4\pi \ell_1 \sin\frac{\theta}{2}}{\lambda}}\right) \qquad (7)$$

where:

ψ_1	is atomic scattering power of oxygen, or square root of scattering cross section of oxygen atom
ψ_2	is atomic scattering power of carbon, or square root of scattering cross section of carbon atom
ℓ_1	is distance between oxygen nuclei in the molecule
ℓ_2	is distance between oxygen and carbon nuclei in the molecule
θ	is angle between incident and scattered waves
λ	is de Broglie wave length of the neutrons
K_1	is normalizing factor, and equals $\dfrac{1}{2\psi_1^2 + \psi_2^2}$
K_2	is normalizing factor, and equals $\dfrac{1}{2\psi_1^2}$

Using equations (6) and (7), curves of I versus θ (for $\theta = 0^\circ$ to 90°) have been calculated. The following values for the constants have been assumed: $\psi_1 = \sqrt{3.9} \times 10^{-12}$ cm., $\psi_2 = \sqrt{4.7} \times 10^{-12}$cm. (see last section), $\ell_1 = 1.20 \times 10^{-8}$cm. (17), $\ell_2 = 1.16 \times 10^{-8}$cm. (18): $\lambda = 1.06 \times 10^{-8}$cm. This wavelength corresponds to a neutron energy of 0.070 e.v. for in the non-relativistic case (10):

$$\lambda = \frac{h}{mv} = \frac{h}{\sqrt{2mE}} \qquad (8)$$

where:

λ is de Broglie wave length of particle in cm.

m is particle mass in gms.

v is particle velocity in cm/sec.

E is particle energy in ergs

h is Planck's constant

(ii) Doppler Correction

The above calculations are for the ideal case of monochromatic neutrons. However in practice the thermal motion of the gas molecules produces a Doppler spread in the neutron wavelength. The effect is small for, the molecule to neutron mass ratio being high, the velocity ratio is low. An approximate correction has therefore been computed by treating separately five equal groups of molecules with component velocities in the direction of the incident neutron beam of 0, $\pm v_1$, $\pm v_2$ (cm./sec., where from kinetic theory (19):

$$\frac{2}{\sqrt{\pi}} \int_0^{\frac{v_1}{\alpha}} e^{-\left(\frac{v_1}{\alpha}\right)^2} d\left(\frac{v_1}{\alpha}\right) = 0.4 \qquad (9)$$

and

$$\frac{2}{\sqrt{\pi}} \int_0^{\frac{v_2}{\alpha}} e^{-\left(\frac{v_2}{\alpha}\right)^2} d\left(\frac{v_2}{\alpha}\right) = 0.8 \qquad (10)$$

α is the most probable molecular velocity (cm./sec.).

From (9) and (10)

$$v_1 = 0.371\alpha \quad \text{and} \quad v_2 = 0.906\alpha$$

Now

$$\alpha = \sqrt{\frac{2RT}{M}} \qquad (11)$$

where: R is gas constant 8.31×10^7 erg/degree/mole.

M is molecular weight of gas

T is absolute temperature of gas

Equations (9), (10) and (11) therefore give the component velocities of each group of molecules. Since the relative velocity of a 0.07 e.v. beam of neutrons with respect to each group is v, $v(1 \pm \frac{v_1}{v})$, $v(1 \pm \frac{v_2}{v})$, where v is the neutron velocity from equation (8), five separate wavelengths may be calculated by substitution back into equation (8). Separate patterns can then be calculated for each group which will be similar in form but expanded or contracted in the θ dimension. These groups of molecules differ only in their velocity component parallel to the neutron beam. Consider now each group to be made up of five equal sub-groups with velocity components of 0, $\pm v_1$, $\pm v_2$ perpendicular to the neutron beam. The patterns of the sub-groups will then be identical in form but displaced in angle from the central position: $0, \pm \frac{v_1}{v}$ and $\pm \frac{v_2}{v}$. The direct addition of these twenty patterns (times a normalizing 0.05) gives the final pattern. In practice it was possible to add the five parallel component patterns and apply the perpendicular component correction to the resultant.

(iii) Change of Coordinate System

The above calculations are for a centre-of-mass system. Since they assume elastic scattering, the conversion to the laboratory system is easily made (20). If:

$$I(\phi) = g(\phi)\ I(\theta) \qquad (12)$$

where: θ is scattering angle in centre-of-mass system

ϕ is scattering angle in laboratory system

$I(\phi)$ and $I(\theta)$ are intensities in two systems

then

$$\theta = \phi + \sin^{-1}\left(\frac{m_2}{m_1} \sin \phi\right) \qquad (13)$$

$$g(\phi) = \frac{\left(\frac{m_2}{m_1} \cos \phi + \sqrt{1 - \left(\frac{m_2}{m_1}\right)^2 \sin^2\phi}\right)^2}{\sqrt{1 - \left(\frac{m_2}{m_1}\right)^2 \sin^2\phi}} \qquad (14)$$

where m_1 and m_2 are masses of scattering and scattered particles. These can be reduced in the case $m_1 \gg m_2$ to:

$$\theta \approx \phi + \frac{m_2}{m_1} \sin \phi \qquad (15)$$

$$g(\phi) \approx 1 + 2 \frac{m_2}{m_1} \cos \phi \qquad (16)$$

Equations (12), (15) and (16) have been applied to the Doppler corrected curves of both CO_2 and O_2. The resultant patterns are plotted in Figures 3 and 4 together with the experimental points from Tables 7 and 8. In addition, to show the magnitudes of the Doppler effect and this conversion, the uncorrected curves for O_2 are given dotted on the same figure (Fig. 4).

FIGURE 3

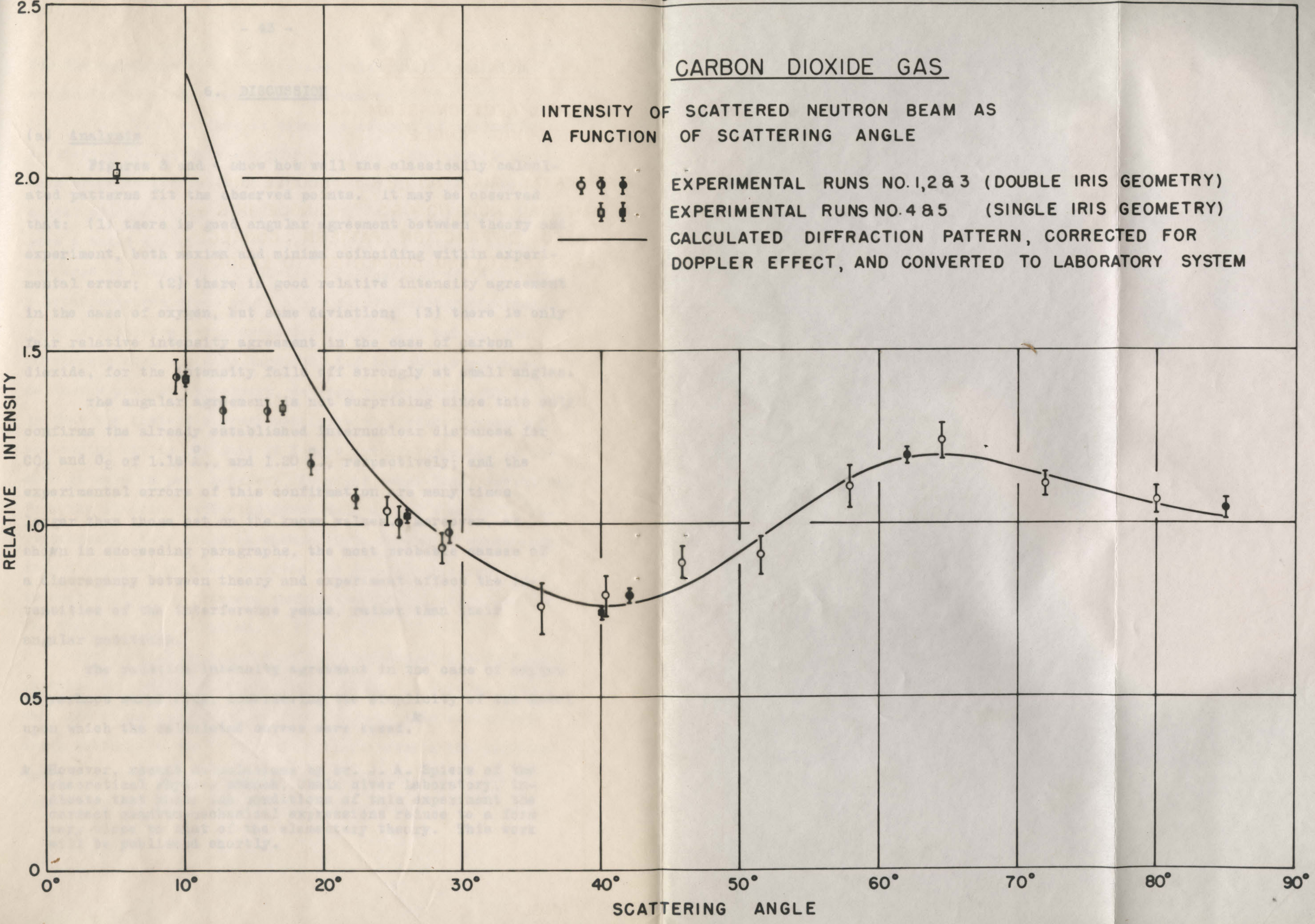
CARBON DIOXIDE GAS
INTENSITY OF SCATTERED NEUTRON BEAM AS A FUNCTION OF SCATTERING ANGLE
EXPERIMENTAL RUNS NO. 1, 2 & 3 (DOUBLE IRIS GEOMETRY)
EXPERIMENTAL RUNS NO. 4 & 5 (SINGLE IRIS GEOMETRY)
CALCULATED DIFFRACTION PATTERN, CORRECTED FOR DOPPLER EFFECT, AND CONVERTED TO LABORATORY SYSTEM
RELATIVE INTENSITY
2.5
2.0
1.5
1.0
0.5
0
0°
10°
20°
30°
40°
50°
60°
70°
80°
90°
SCATTERING ANGLE

FIGURE 4

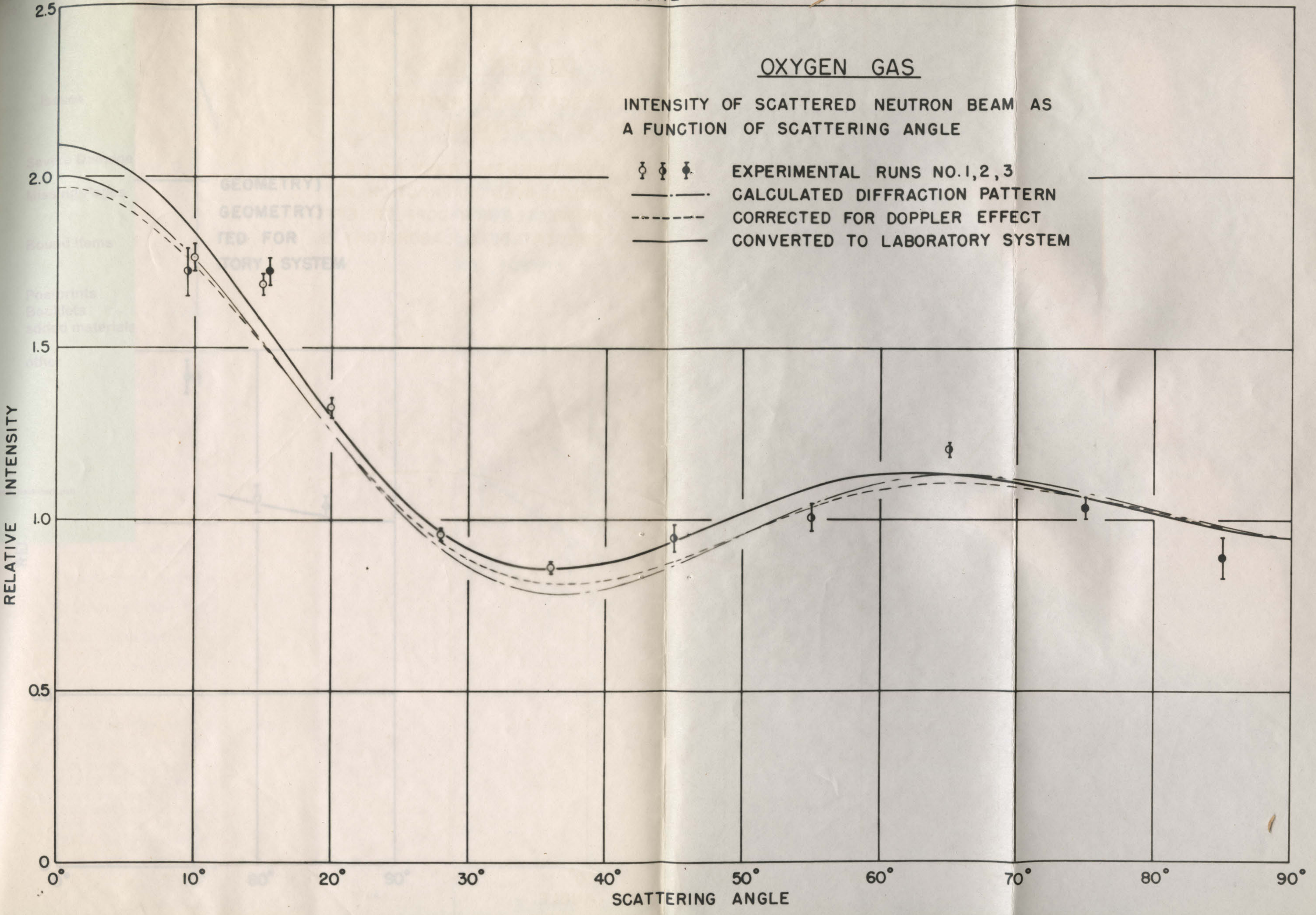
OXYGEN GAS
INTENSITY OF SCATTERED NEUTRON BEAM AS A FUNCTION OF SCATTERING ANGLE
EXPERIMENTAL RUNS NO. 1, 2, 3
CALCULATED DIFFRACTION PATTERN
CORRECTED FOR DOPPLER EFFECT
CONVERTED TO LABORATORY SYSTEM
RELATIVE INTENSITY
2.5
2.0
1.5
1.0
0.5
0
0°
10°
20°
30°
40°
50°
60°
70°
80°
90°
SCATTERING ANGLE

6. DISCUSSION

(a) Analysis

Figures 3 and 4 show how well the classically calculated patterns fit the observed points. It may be observed that: (1) there is good angular agreement between theory and experiment, both maxima and minima coinciding within experimental error; (2) there is good relative intensity agreement in the case of oxygen, but some deviation; (3) there is only fair relative intensity agreement in the case of carbon dioxide, for the intensity falls off strongly at small angles.

The angular agreement is not surprising since this only confirms the already established internuclear distances for CO_2 and O_2 of 1.16 Å., and 1.20 Å., respectively; and the experimental errors of this confirmation are many times larger than those set on the known values. Moreover, as shown in succeeding paragraphs, the most probable causes of a discrepancy between theory and experiment affect the intensities of the interference peaks, rather than their angular positions.

The relative intensity agreement in the case of oxygen is perhaps surprising, considering the simplicity of the model upon which the calculated curves were based.*

---

* However, recent calculations by Dr. J. A. Spiers of the Theoretical Physics Branch, Chalk River Laboratory, indicate that under the conditions of this experiment the correct quantum-mechanical expressions reduce to a form very close to that of the elementary theory. This work will be published shortly.

For the model has two inadequacies which could cause discrepancies between theory and experiment.

The first is that it takes no account of inelastic scattering though this is known to occur. The magnitude of this error is difficult to estimate, but there is experimental evidence that it may be small. Fermi and Marshall (9) give a total measured cross section for CO_2 of 24.5 barns compared to a calculated elastic cross section of 24.8 barns, a total measured cross section for O_2 of 16.2 barns compared to a calculated elastic cross section of 13.2 barns. The wavelength used was very long (5.1 Å.) but the gases were, as in the present experiment, at room temperature. It is likely that the inelastic cross section will produce incoherent scattering (as in the case of X-rays and electrons). If however it were in part coherent, it might cause local deviations from the elastic scattering curve such as are observed. Experimentally this could be checked by a series of measurements over a range of neutron energies and gas temperatures; theoretically by a rigorous quantum-mechanical calculation of the inelastic contribution.

The second inadequacy of the theoretical model is that it takes no account of the magnetic moment of oxygen. Since this gas is paramagnetic, part of its molecular scattering cross section is due to the interaction between the magnetic moments of the oxygen molecules and neutrons (21). The effect however can introduce only incoherent scattering (22), and since this has not been observed, it would appear to be small.

Since the oxygen correlation is so good, inadequacy of the theoretical model cannot easily explain the lack of relative intensity agreement in the case of carbon dioxide. More probable is intermolecular interference from molecules that are not completely free. In a study of X-ray scattering from argon near its liquid phase, Eisenstein and Gingrich (23) have shown that the gas pattern exhibits interference features characteristic of the liquid pattern. Earlier Debye (24) had shown theoretically that a monatomic gas at very high pressure should give an interference minimum due to an intermolecular distance regularity introduced by the actual volume of the molecules. This cannot explain the results found in the argon study however, since the argon density was in general much less than that assumed by Debye. An analysis by Vineyard (25) indicates that partial association of the argon molecules, giving rise to density fluctuations in the vapour, might explain the patterns observed by Eisenstein and Gingrich. If the carbon dioxide experimental diffraction pattern (Fig. 3) is compared with the equivalent* argon diffraction pattern (curves 8, 19, 22) (23), it is found that the deficiency in scattering is in good agreement but that the carbon dioxide shows no excess scattering corresponding to the liquid peak found for argon.

* By the Law of Corresponding States

The evidence is therefore good but inconclusive that the intensity deficiency in the CO_2 pattern is due to the gas being near the liquid phase.

(b) Errors

Experimental limits on the points of Figures 3 and 4 are standard deviations due only to counting statistics. To this uncertainty must be added any experimental errors.

(1) Temperature and pressure - Where no temperature was taken there could be a $1^{\circ}C$ error, or $\sim$ 0.8% uncertainty in the density of the carbon dioxide. With the Airco pressure gauge, a 2% pressure uncertainty or $\sim$ 3.6% density uncertainty is possible.

(2) Gas purity - Electrolytic oxygen is 99.6% pure, so that even a hydrogen impurity could not seriously affect the results. Impurities in CO_2 are probably larger (26). A 1% H_2 contamination could cause a 10% incoherent background, but in the laboratory system this background would be larger rather than smaller at small scattering angles, in contrast to the observed intensities. Hydrogenous gases could be serious if their abundances were appreciable, (say $>$ 1%), but this is unlikely. Other gaseous impurities can be neglected since their scattering cross sections are not appreciably greater than that of carbon dioxide.

(3) Energy and angular spread of incident beam - The former is due partly to crystal disorder, but mainly to the solid

angle of the primary beam. Width of primary beam $\Delta\theta = \pm 1/3^{\circ}$, so variation in neutron wave length

$$\Delta\lambda = \pm\frac{1}{3} \times \frac{1}{11} = \pm 3\%.$$

The result is a negligible flattening of the pattern, analogously to the Doppler broadening. The finite beam width has a similar effect.

(4) Higher orders - Measurements and calculations by D. G. Hurst show 2nd and higher orders to be $<$ 2% at 0.07 e.v. energy.

(5) Chamber asymmetry - With the variation $<$ 0.001" in 0.080", and the wall attenuation $\sim$ 20%, the intensity error must be $<$ 0.3%.

(6) Iris widths and alignment - It can be shown that misalignment has no effect to a first order of accuracy. From 90° to 30° the same is true of a variation in nominal slit width, but at 0° there may be an error in scattered intensity proportional to this variation. The measured variation was 0.012" or 2-1/2% of 0.500", so at small angles a 1-1.5% error is possible from this cause.

(7) Multiple scattering - Since gas and wall do not scatter isotropically as assumed for this correction, this is a possible source of error. It does not easily explain differences in the behaviour of CO_2 and O_2. But since the wall does scatter with pronounced interference peaks, it could explain small peaks which both gases have in common such as at 16°.

(8) Background - This correction is subject to criticism on several counts. Firstly, the averaging procedure for CO_2 may not be completely justified, i.e. measurements of fast neutron background should be taken at every point. However an error introduced in this way could not be large, for such a fast neutron background cannot have rapid variations in angle. Secondly, the attenuation correction is not independent of angle. Such an error will appear at the larger angles, but fortunately at these angles the correction is small, e.g. if O_2 attenuation at 65° is one half that shown in Table 8, the resultant error in intensity is 1.2%, or less than the standard deviation. Finally, constancy of background may be questioned. Night and week-end runs largely overcame this difficulty but run 3 of oxygen (75° and 85°) was made during the day, and is suspect on that count. The error at these angles might be as high as 5 - 10% due to stray radiation from neighbouring beam experiments. And finally it was noted (under "Apparatus") that counter 2 was unchecked for γ-sensitivity. However, a γ- background would be measured with the fast neutrons so its subtraction is assured.

(c) Recommendations

Recommendations for future gas scattering experiments fall into three categories: (1) improvements in experimental technique; (2) companion theoretical studies; (3) targets most usefully investigated.

In the first category looms large the reduction of background and double scattering. Heavier shielding about the primary beam, and around the collimators and counter is indicated. This point is in fact a major consideration in a newly designed monochromatizer being built by the Technical Physics group. Double scattering can be reduced in several ways. A decrease in pressure or in iris height reduces the gas-gas component, but at the expense of intensity, therefore unprofitably. A reduction in wall thickness through the use of high stress steel reduces the gas-wall and wall-gas components at no sacrifice. Further, internal shielding of three quadrants with cadmium reduces the gas-wall component still more. By these means an overall double-to-single scattering ratio of 3% might be achieved.

Categories two and three go hand in hand. It has been suggested already that further investigation might well be done on the same two gases, over a range of temperatures, pressures and neutron energies. This should throw light on the irregularities observed. The investigation would require many months, even with shortened runs through an improved technique. At a later date this should be done, but immediately it may be of more value to perform experiments specifically designed to yield useful information with one or two patterns. Such experiments lean heavily on theory. What are some of these experiments?

One might be scattering of neutrons by deuterium gas (at the temperature of liquid air, to reduce Doppler effect). There is good evidence that the neutron-deuteron scattering cross section is spin dependent, but accurate values of the two scattering amplitudes have not been determined. (12), (27), (13) A calculation based on Schwinger-Teller theory (28) will show whether the differential cross section depends markedly on these amplitudes, and therefore whether there is value in an angular distribution measurement. This problem is being investigated in the Theoretical Physics Branch under Dr. W. H. Watson, at Chalk River.

Another might be the scattering of neutrons by nitrogen. This nucleus too is spin dependent (27), and has the great advantage of occurring naturally as almost a single isotope. Once again, a theoretical treatment is desirable.

And finally there is the scattering by oxygen. If a rigorous calculation could be done on this gas (perhaps at liquid nitrogen or hydrogen temperatures where fewer rotational states are involved) then one or two patterns might yield data on the magnetic interaction between neutron and nucleus.

APPENDIX

Double Scattering

General Case

Consider Fig.1A(a) where:

R,t,T,W,w and T are internal radius, wall thickness, widths and height of incident and finally scattered beams, respectively

x,y,z are coordinates of incident beam

x',y',z' are coordinates of finally scattered beam

ϕ is angle between coordinate systems x,y,z and x',y',z'

$L(x,y,z,x',y',z',\phi)$ is distance between x,y,z and x',y',z'

$\theta_1(x,y,z,x',y',z',\phi)$ is angle between incident and singly scattered beam

$\theta_2(x,y,z,x',y',z',\phi)$ is angle between singly and doubly scattered beam

N is intensity of incident beam (neutrons/sec./cm^2)

$\varepsilon(\theta)$ is fraction of beam scattered by gas/unit length/unit solid angle as a function of scattering angle θ

$\mu(\theta)$ is fraction of beam scattered by wall/unit length/unit solid angle as a function of scattering angle θ

η is solid angle of final beam

If only a small fraction of the beam is scattered by gas and wall, the intensity of singly scattered beam is:

$$n(\phi) \approx NWTw\eta \frac{\varepsilon(\phi)}{\sin\phi} \qquad \left(\text{for } \phi \nless \sin^{-1}\frac{W}{2R} + \sin^{-1}\frac{w}{2R}\right) \tag{A1}$$

and doubly scattered beam is:

$$n(\phi) \approx N\eta \Bigg\{ \int_{-\frac{W}{2}}^{\frac{W}{2}} \int_{-\sqrt{R^2-x^2}}^{\sqrt{R^2-x^2}} \int_{-\frac{T}{2}}^{\frac{T}{2}} \int_{-\frac{w}{2}}^{\frac{w}{2}} \int_{-\sqrt{R^2-x'^2}}^{\sqrt{R^2-x'^2}} \int_{-\frac{T}{2}}^{\frac{T}{2}} \frac{\varepsilon(\theta_1)\,\varepsilon(\theta_2)}{L^2}\, dx\, dy\, dz\, dx'\, dy'\, dz'$$

$$+ \int_{-\frac{W}{2}}^{\frac{W}{2}} \int_{\substack{+\sqrt{R^2-x^2} \\ -\sqrt{(R+t)^2-x^2}}}^{\substack{+\sqrt{(R+t)^2-x^2} \\ -\sqrt{R^2-x^2}}} \int_{-\frac{T}{2}}^{\frac{T}{2}} \int_{-\frac{w}{2}}^{\frac{w}{2}} \int_{-\sqrt{R^2-x'^2}}^{\sqrt{R^2-x'^2}} \int_{-\frac{T}{2}}^{\frac{T}{2}} \frac{\mu(\theta_1)\,\varepsilon(\theta_2)}{L^2}\, dx\, dy\, dz\, dx'\, dy'\, dz'$$

$$+ \int_{-\frac{W}{2}}^{\frac{W}{2}} \int_{-\sqrt{R^2-x^2}}^{\sqrt{R^2-x^2}} \int_{-\frac{T}{2}}^{\frac{T}{2}} \int_{-\frac{w}{2}}^{\frac{w}{2}} \int_{\substack{+\sqrt{R-x'^2} \\ -\sqrt{(R+t)^2-x'^2}}}^{\substack{+\sqrt{(R+t)^2-x'^2} \\ -\sqrt{R-x'^2}}} \int_{-\frac{T}{2}}^{\frac{T}{2}} \frac{\varepsilon(\theta_1)\,\mu(\theta_2)}{L^2}\, dx\, dy\, dz\, dx'\, dy'\, dz' \Bigg\} \tag{A2}$$

For explicit values of the functions $\varepsilon(\theta)$ and $\mu(\theta)$ this integral expression can be evaluated numerically. This has been done for special cases.

<u>Case I</u>

$W < R \quad w < R$ and $t \ll R$ (see Fig. A1 (b))

In addition, the gas and wall are assumed to scatter isotropically:

$$\varepsilon = \frac{\varepsilon_1}{4\pi} \text{ and } \mu = \frac{\mu_1}{4\pi}$$

Then, the intensity of singly scattered beam is:

$$N(\phi) \approx \frac{NWTw\,\varepsilon_1\eta}{4\pi \sin\phi} \quad (\text{for } \phi \nless \sin \frac{W}{2R} + \sin^{-1}\frac{w}{2R}) \qquad (A3)$$

and doubly scattered beam is:

$$N(\phi) \approx \frac{N\varepsilon_1\eta}{16\pi^2}\left\{\varepsilon_1 \int_{-\frac{W}{2}}^{\frac{W}{2}}\int_{-R}^{R}\int_{-\frac{T}{2}}^{\frac{T}{2}}\int_{-\frac{w}{2}}^{\frac{w}{2}}\int_{-R}^{R}\int_{-\frac{T}{2}}^{\frac{T}{2}} \frac{1}{L^2}\, dxdydzdx'dy'dz' \right.$$

$$\left. + 4\mu_1 t \int_{-\frac{W}{2}}^{\frac{W}{2}}\int_{-\frac{T}{2}}^{\frac{T}{2}}\int_{-\frac{w}{2}}^{\frac{w}{2}}\int_{-R}^{R}\int_{-\frac{T}{2}}^{\frac{T}{2}} \frac{1}{L^2}\, dxdzdx'dy'dz' \right\} \qquad (A4)$$

Letting ratio of intensities of doubly to singly scattered beam be $M(\phi)$, and replacing continuous variables x,y,z, x',y',z' with integers ℓ,m,n, ℓ',m',n', respectively, gives:

$$M(\phi) \approx \frac{\sin\phi}{4\pi WTw}\left\{\varepsilon_1 \sum_{\ell=1}^{W}\sum_{m=1}^{2R}\sum_{n=1}^{T}\sum_{\ell'=1}^{w}\sum_{m'=1}^{2R}\sum_{n'=1}^{T} \frac{\Delta\ell\Delta m\Delta n\Delta\ell'\Delta m'\Delta n'}{L^2(\ell,m,n,\ell',m',n')}\right.$$

$$\left. + 4\mu_1 t \sum_{\ell=1}^{W}\sum_{n=1}^{T}\sum_{\ell'=1}^{w}\sum_{m'=1}^{2R}\sum_{n'=1}^{T} \frac{\Delta\ell\Delta n\Delta\ell'\Delta m'\Delta n'}{L^2(\ell,n,\ell',m',n')}\right\}$$

$$(\text{for } \phi \nless \sin^{-1}\frac{W}{2R} + \sin^{-1}\frac{w}{2R}) \qquad (A5)$$

Note

In the following numerical examples: (1) The wall is assumed to scatter isotropically only for $\pi/6 < \theta < \pi$, not at all for $0 < \theta < \pi/6$; therefore all values of 1/L having ℓ',m',n' within this 60° cone are omitted from the summation. (2) The value of $1/L^2$ for $\ell,m,n \equiv \ell',m',n'$ has been determined by further numerical integration to be approximately 5.0 for double scattering from gas, 3.0 for double scattering from wall.

Examples

$W = w = 1.27$ cm.; $R = T = 2.54$ cm.

$$\varepsilon_1 = \begin{cases} .0258/\text{cm. for } CO_2 \text{ at 775 p.s.i., } 22.3^\circ C. \\ .0116/\text{cm. for } O_2 \text{ at 910 p.s.i., } 22.3^\circ C. \end{cases}$$

$\mu_1 t = 0.197$ (for a 0.203 cm. iron wall)

Let unit of length be 1/4" for summations in equation (A5), then:

$$W = w = 2;\ R = T = 4;\ \varepsilon_1 = \begin{cases} .0164/\text{unit length or} \\ .0074/\text{unit length} \end{cases};\ \mu_1 t = 0.197$$

and equation is valid for $\phi > 29^\circ$

(a) $\phi = 90^\circ$

$$M = \frac{1}{4\pi x 2 x 4 x 2}\left\{8\varepsilon_1 \sum_{l=1}^{2}\sum_{m=1}^{4}\sum_{n=1}^{2}\sum_{l'=1}^{2}\sum_{m'=1}^{4}\sum_{n'=1}^{4}\frac{1}{L^2} + 16\mu_1 t \sum_{n=1}^{2}\sum_{l'=1}^{2}\sum_{m'=1}^{8}\sum_{n'=1}^{4}\frac{1}{L^2}\right\}$$

$= 3.07\,\varepsilon_1 + .053$ or 10.3% for CO_2, 7.6% for O_2

(b) $\phi = 45^\circ$

$$M = \frac{0.707}{4\pi x 2 x 4 x 2}\left\{4\varepsilon_1 \sum_{l=1}^{2}\sum_{m=1}^{4}\sum_{n=1}^{2}\sum_{l'=1}^{2}\sum_{m'=1}^{8}\sum_{n'=1}^{4}\frac{1}{L^2} + 8\mu_1 t \sum_{l=1}^{2}\sum_{n=1}^{2}\sum_{l'=1}^{2}\sum_{m'=1}^{8}\sum_{n'=1}^{4}\frac{1}{L^2}\right\}$$

$= 2.40\,\varepsilon_1 + .046$ or 8.5% for CO_2, 6.4% for O_2

(c) $\phi = 0^\circ$ ($\frac{\sin\phi}{w}$ replaced by $\frac{1}{2R}$; see singly scattered beam, Case II)

$$M = \frac{1}{4\pi x 2 x 4 x 8}\left\{8\varepsilon_1 \sum_{m=1}^{4}\sum_{n=1}^{2}\sum_{l'=1}^{2}\sum_{m'=1}^{8}\sum_{n'=1}^{4}\frac{1}{L^2} + 16\mu_1 t \sum_{n=1}^{2}\sum_{l'=1}^{2}\sum_{m'=1}^{8}\sum_{n'=1}^{4}\frac{1}{L^2}\right\}$$

$= 1.44\,\varepsilon_1 + .063$ or 8.7% for CO_2, 7.4% for O_2

Case II

$W < R \quad w \not< 2(R+t) \quad t \ll R$ (see Fig. A1(c))

Gas and wall assumed to scatter isotropically:*

$$\varepsilon = \frac{\varepsilon_1}{4\pi} \text{ and } \mu = \frac{\mu_1}{4\pi}$$

Then intensity of singly scattered beam is:

$$n \approx \frac{NWTR\,\varepsilon_1\eta}{2\pi} \qquad (A6)$$

and doubly scattered beam:

$$n(\phi) \approx \frac{N\varepsilon_1\eta}{16\pi^2}\left\{\varepsilon_1 \int_{-\frac{W}{2}}^{\frac{W}{2}}\int_{-R}^{R}\int_{-\frac{T}{2}}^{\frac{T}{2}}\int_{-R}^{R}\int_{-\sqrt{R^2-x'^2}}^{\sqrt{R^2-x'^2}}\int_{-\frac{T}{2}}^{\frac{T}{2}} \frac{1}{L^2}\,dx\,dy\,dz\,dx'dy'dz'\right.$$

$$+\,2\mu_1 t \int_{-\frac{W}{2}}^{\frac{W}{2}}\int_{-\frac{T}{2}}^{\frac{T}{2}}\int_{-R}^{R}\int_{-\sqrt{R^2-x'^2}}^{\sqrt{R^2-x'^2}}\int_{-\frac{T}{2}}^{\frac{T}{2}} \frac{1}{L^2}\,dx\,dz\,dx'dy'dz'$$

$$\left.+\,\mu_1 \int_{-\frac{W}{2}}^{\frac{W}{2}}\int_{-R}^{R}\int_{-\frac{T}{2}}^{\frac{T}{2}}\int_{-(R+t)}^{R+t}\int\limits_{\substack{\sqrt{R^2-x'^2}\\ -\sqrt{(R+t)^2-x'^2}}}^{\substack{\sqrt{(R+t)^2-x'^2}\\ -\sqrt{R^2-x'^2}}}\int_{-\frac{T}{2}}^{\frac{T}{2}} \frac{1}{L^2}\,dx\,dy\,dz\,dx'dy'dz'\right\}$$

(A7)

The ratio of intensities of doubly to singly scattered beam $(M(\phi))$ can be evaluated numerically: but the expression is not as simple as equation (A5), since the summation extends over the whole cylindrical volume of gas and wall. Fortunately the first two terms of equation (A7) are independent of ϕ.

* Qualified for numerical example as in Case I

Using the data of Case I, the value of M for CO_2 has been determined. The third term was calculated for $\phi = 0^o$, but an estimate for $\phi = 30^0$ shows it to be very nearly constant over this range. An average value is given

$$M = .042 + .066 + 0.104 = 21.2\%$$

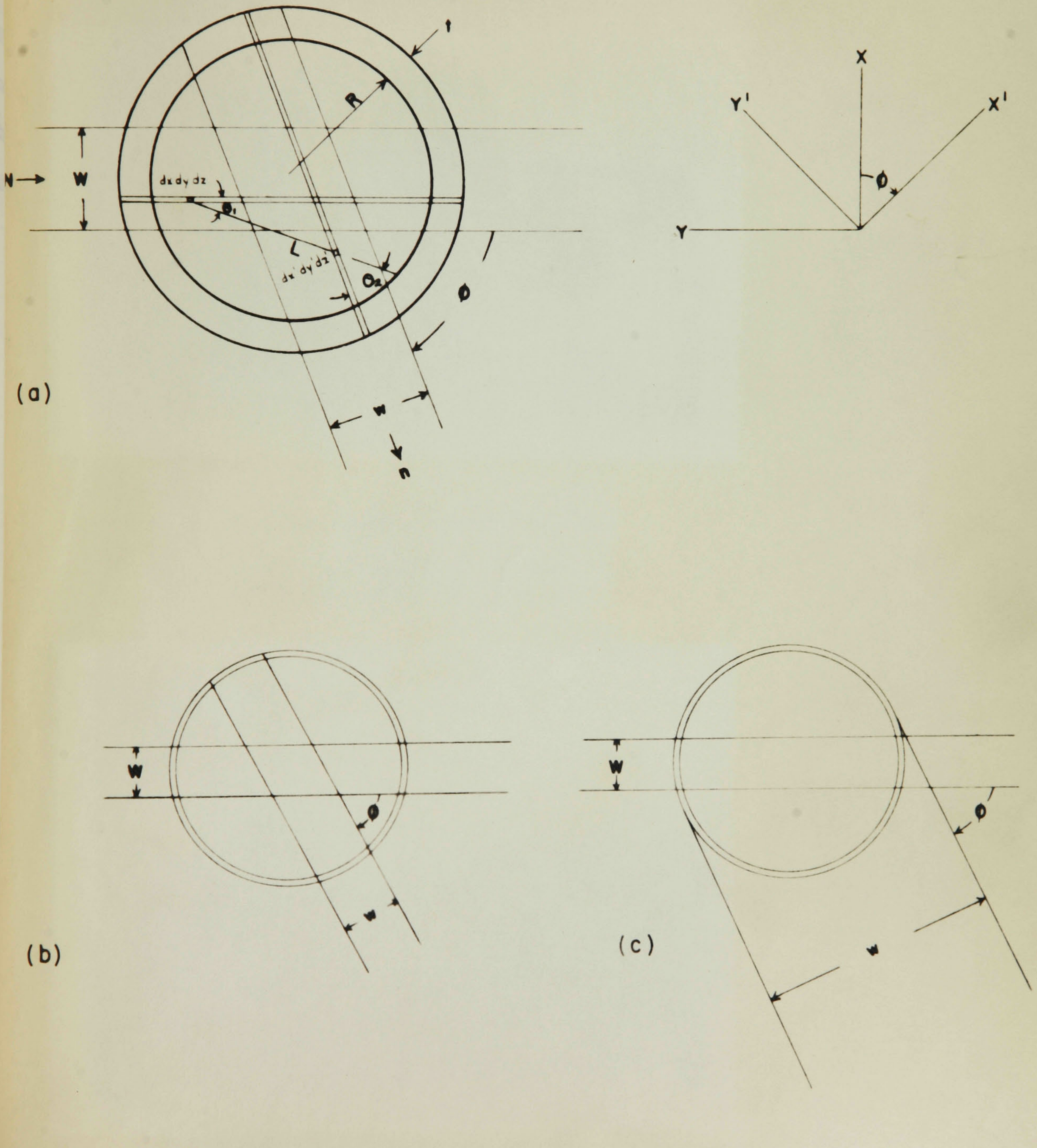

FIGURE A1 — DOUBLE SCATTERING

PHOTOGRAPHS

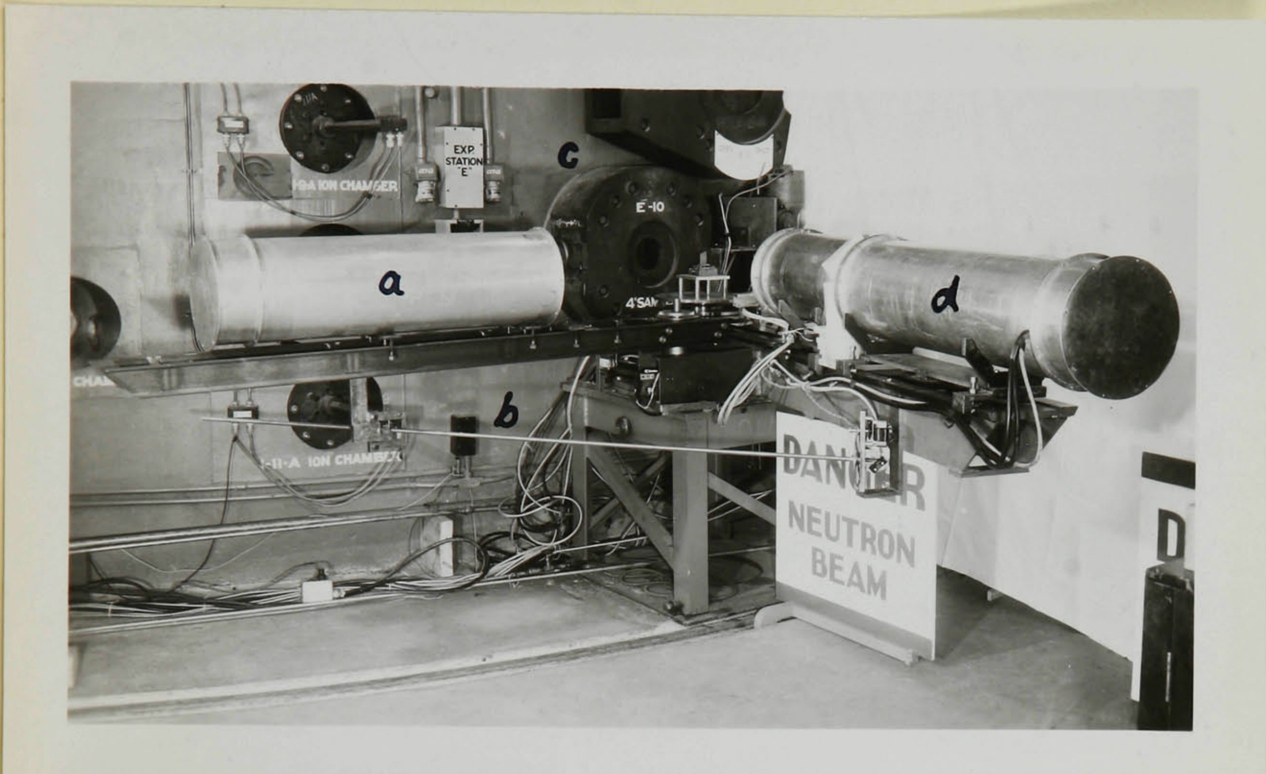

(a) BF_3 counter and shield

(b) Drive shaft

(c) Experimental hole E-10

(d) Auxiliary BF_3 counter (not used)

1. Neutron Crystal Spectrometer

(with gas chamber, collimators, and beam catcher removed)

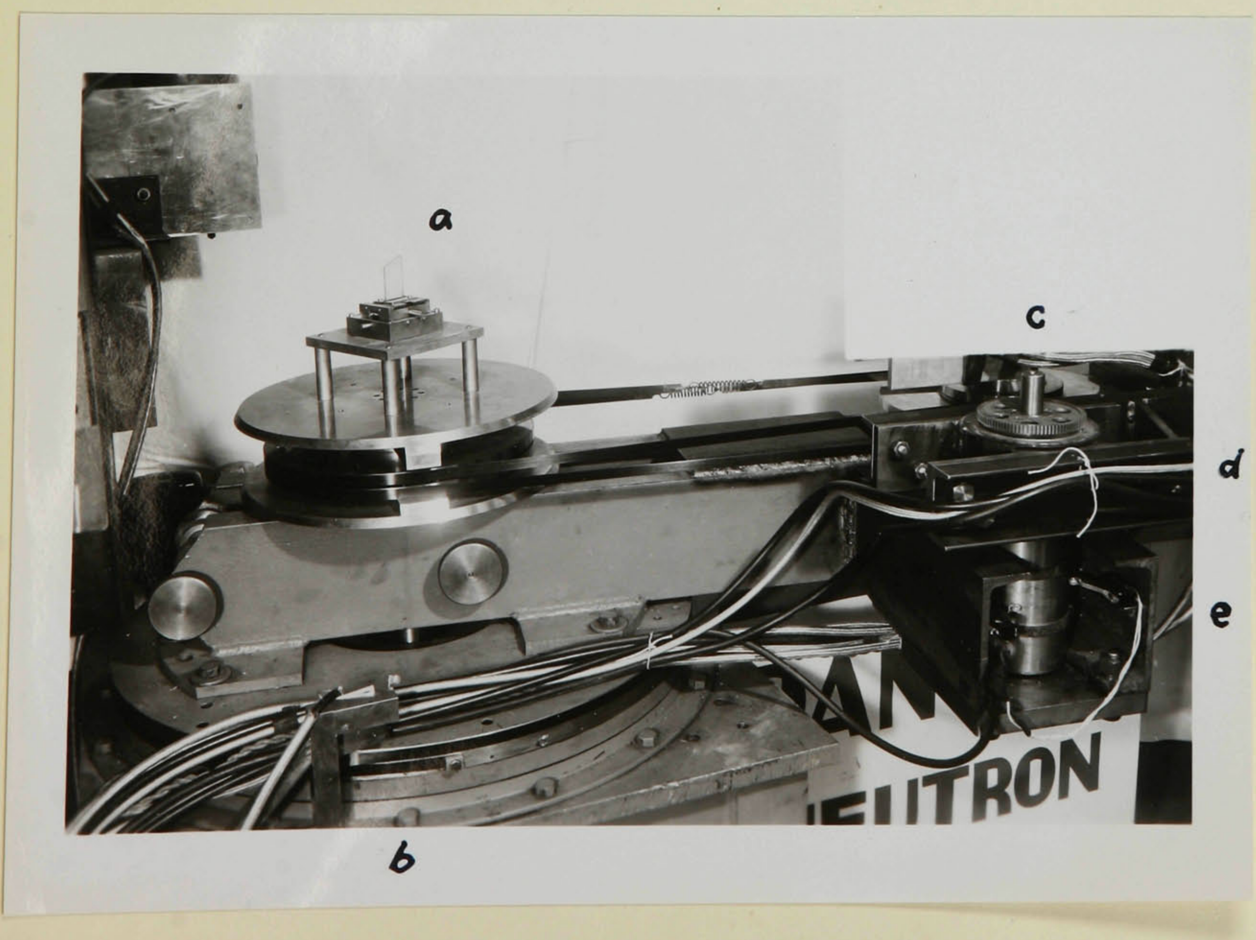

(a) NaCl crystal

(b) Bofors turn-table

(c) Gas chamber mounting post

(d) Counter arm

(e) Limit switches

2. Crystal Assembly Detail

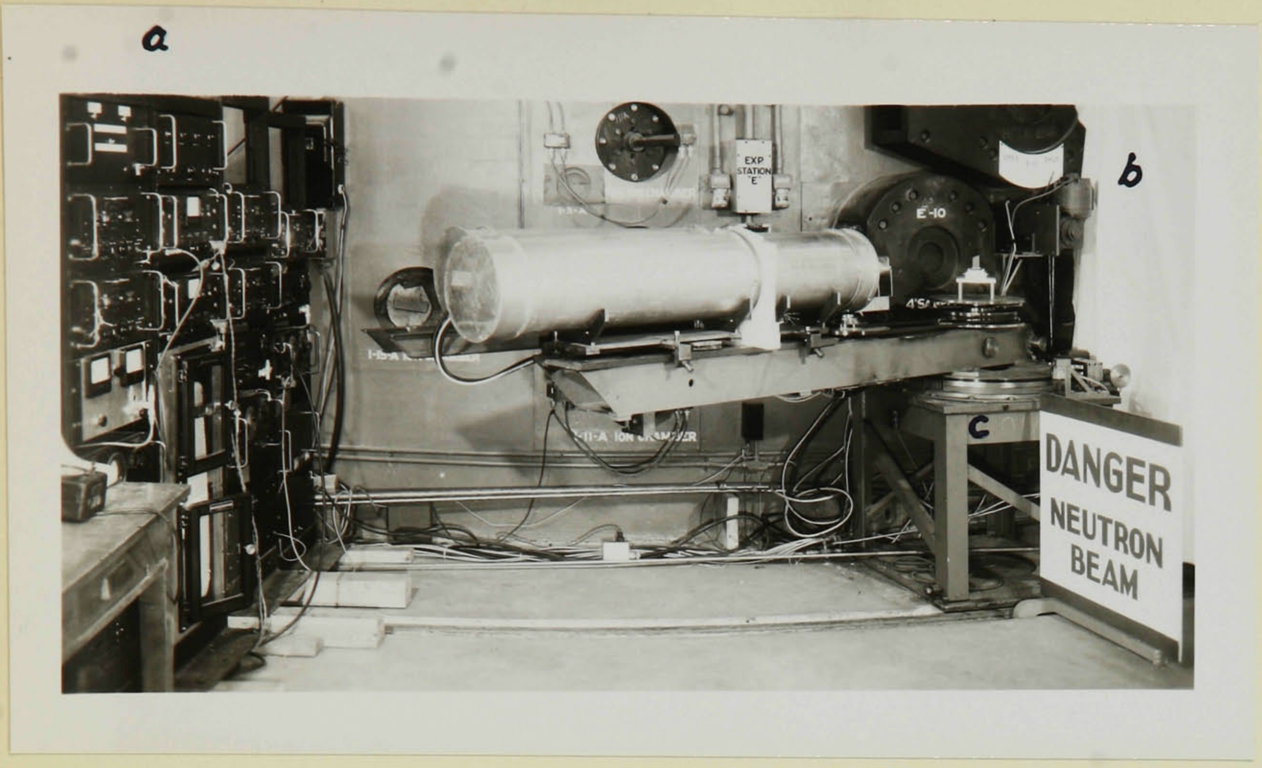

(a) Associated electrical equipment

(b) Beam shutter motor control

(c) Bofors turntable

3. Spectrometer and Associated Electrical Equipment

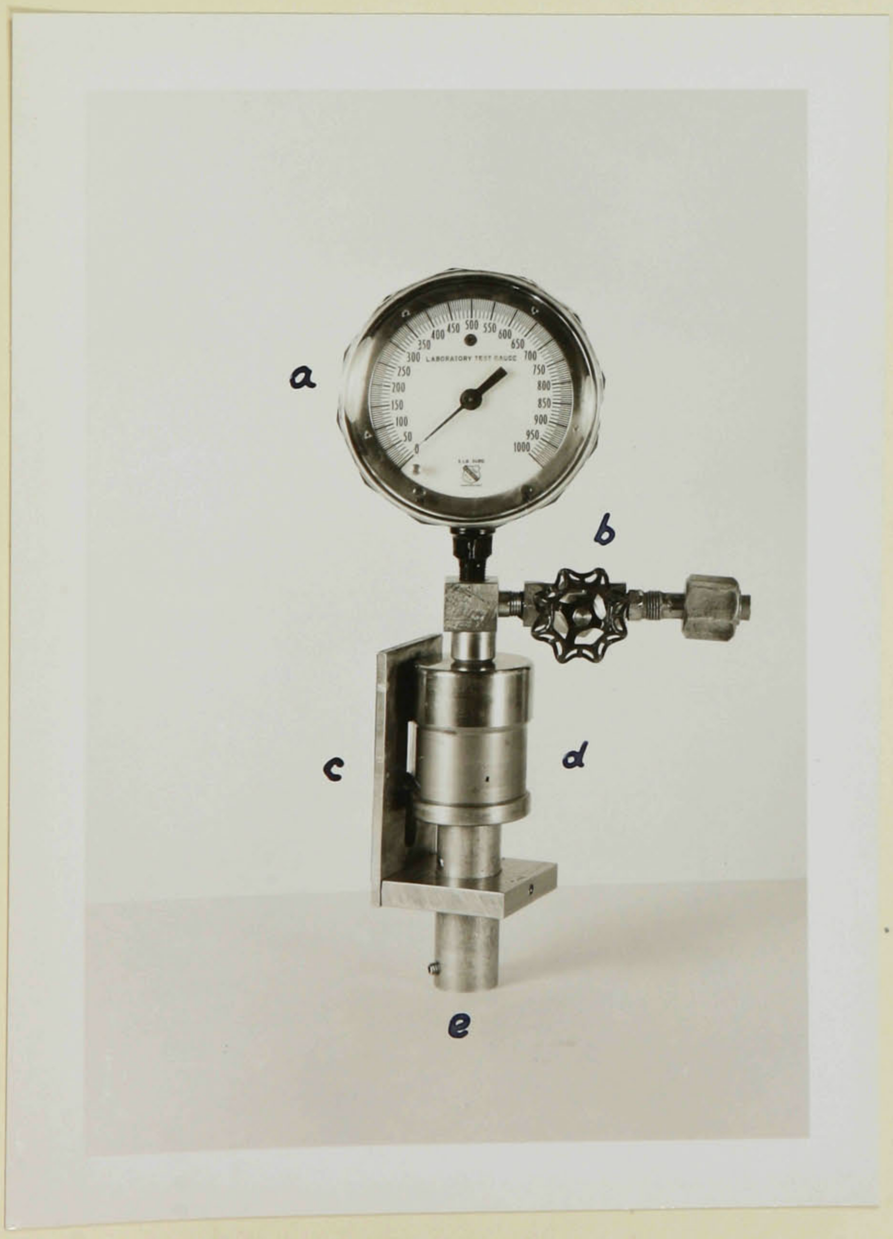

(a) Pressure gauge

(b) Needle valve

(c) Cadmium iris

(d) Gas chamber

(e) Mounting coupling (see photo.2(c))

4. Gas Chamber

BIBLIOGRAPHY

(1) P. Debye, L. Bewilogua, F. Ehrhardt, Physik. Zeits. 30, 84 (1929).

(2) P. Debye, Ann. Phys. Lpz. 46, 809 (1915).

(3) L. Bewilogua, Physik. Zeits. 32, 265 (1931).

(4) H. Mark and R. Wierl, Zeits. f. Physik. 60, 741 (1930).

(5) R. Wierl, Ann. der Physik, 8, 521 (1931).

(6) c.f. L.O. **Brockway**, Rev. Mod. Phys. 8, 231 (1936).

(7) D.P. Mitchell and P.N. Powers, Phys. Rev. 50, 486 (1936).

(8) W.H. Zinn, Phys. Rev. 70, 102 (1946).

(9) E. Fermi and L. Marshall, Phys. Rev. 71, 666 (1947).

(10) c.f. A.H. Compton and S.K. Allison, "X-Rays in Theory and Experiment" (Van Nostrand Company, Inc., New York, 1940); G.P. Thomson and W. Cochrane, "Theory and Practice of Electron Diffraction" (Macmillan and Company, Ltd., London, 1939); M.H. Pirenne, "Diffraction of X-Rays and Electrons by Free Molecules" (Cambridge University Press, London, 1946).

(11) J. Schwinger and E. Teller, Phys. Rev. 52, 286 (1937).

(12) C.G. Shull, E.O. Wollan, G.A. Morton and W.L. Davidson, Phys. Rev. 73, 842 (1948).

(13) E. Fermi and L. Marshall, Phys. Rev. 75, 578 (1949).

(14) E.L. Quinn and C.L. Jones, "Carbon Dioxide" (Reinhold Publishing Corp., New York, 1936).

(15) H.H. Goldsmith, H.W. Ibser and B.T. Feld, Rev. Mod. Phys. 19, 259 (1947).

(16) C. Goodman, editor, "The Science and Engineering of Nuclear Power, Vol. 1" (Addison-Wesley Press Inc., Cambridge, 1947).

(17) G. Herzberg, "Molecular Spectra and Molecular Structure" (Prentice Hall, Inc., New York, 1939).

(18) G. Herzberg, "Infrared and Raman Spectra" (Van Nostrand Company, Inc., New York, 1944).

(19) c.f. E.H. Kennard, "Kinetic Theory of Gases" (McGraw-Hill Book Company, Inc., New York, 1938).

(20) N. Arley, Det. Kgl. Danske Videnskabernes Selskab. Mathematisk-fysiske Meddelelser. 15, 1 (1938).

(21) E. Melkonian, L.J. Rainwater, W.W. Havens, Jr., and J.R. Dunning, Phys. Rev. 73, 1399 (1948).

(22) O. Halpern, Phys. Rev. 72, 746 (1947).

(23) A. Eisenstein and N.S. Gingrich, Phys. Rev. 62, 261 (1942).

(24) P. Debye, Physik. Zeits. 28, 135 (1927).

(25) G.H. Vineyard, Phys. Rev. 74, 1076 (1948).

(26) A. Farkas and H.W. Melville, "Experimental Methods in Gas Reactions" (Macmillan and Company, Ltd., London, 1939).

(27) C.G. Shull and E.O. Wollan, Bull. of the A.P.S. 24, 1, 31 (1949).

(28) M. Hamermesh and J. Schwinger, Phys. Rev. 69, 145 (1946).